Self-Patterned Growth of Branched Structures in Non-Curing and in Curable Structures via Electro-Hydrodynamic Hele-Shaw Flow

A Thesis

Submitted to the Faculty

of

Drexel University

by

Julia Lynn Cutler

in partial fulfillment of the

requirements for the degree

of

Master of Science in Chemical Engineering

October 2009

Dedications

I dedicate this thesis to those serving in the armed forces of the United States of America. May our work help to keep them safe, while they do the same for each and every one of us.

Acknowledgements

My sincerest thanks go to all of the talented research professionals who have guided and supported me throughout the master's thesis process. I would first like to thank Dr. Giuseppe Palmese, my mentor and research advisor during my five years at Drexel University. Without his enthusiasm and encouragement, completing a BS/MS program would have seemed overly daunting. I would also like to thank Dr. Eric Wetzel, without whom this research project would not have been possible. Dr. Wetzel was the main driver of exploring the possibility of electro-hydrodynamic viscous fingering as a biomimetic branching technique. Dr. Wetzel was invaluable as a mentor and resource for this thesis work.

Many thanks go to the research collaborators both at the Army Research Laboratories at the Aberdeen Proving Grounds, MD and in the Palmese group at Drexel University in Philadelphia, PA. Special thanks to Dr. Kristopher Behler, Phillip Dirlam, Alex Grous, Kevin Andrews, and Minhazuddin Mohammed for their much-appreciated help with my research efforts.

I would also like to thank the professors and staff of the Chemical and Biological Engineering Department at Drexel University. I will forever remember and cherish the time that I spent learning from them.

Table of Contents

List of Tables

List of Figures

Abstract

Self-Patterned Growth of Branched Structures in Non-Curing and in Curable Structures via Electro-Hydrodynamic Hele-Shaw Flow

Julia Lynn Cutler

Dr. Giuseppe R. Palmese

Dr. Eric D. Wetzel

Current research aims to find effective means of creating biomimetic vascular systems for polymeric composite materials. One method for autonomic growth of branching structures is explored in this thesis. Motivation is taken from electrical treeing and viscous fingering phenomena. Applying these basic principles, Saffman-Taylor instability is combined with an applied electrical potential in order to grow and control branching patterns in a curable polymeric system. The goal is to create a finely and complexly branched channel in a variety of matrix media. Increasing the viscosity ratio between the matrix and injection fluid increases the degree of branching and decreases droplet formation from the structure. Adding surfactant to a silicone oil system works to decrease the interfacial tension between these fluids and decreases droplet formation at the expense of some degree of branching. Increasing the voltage applied to the system increases branching, although also increases the amount of droplets. Flow rate must be finely tuned in order to avoid pooling in the channels. These principles hold true in a silicone oil and water system, and are similarly expressed in a curable pre-polymer matrix system. Successful cure of a finely branched system was achieved guided by an understanding of appropriate dimensionless groups describing the relative importance of physical forces. The viability of structures prepared in this way was demonstrated by successfully filling and flowing material through all length scales of branches.

CHAPTER 1: INTRODUCTION

1.1 Motivation

Many researchers are currently exploring polymerized vascular systems for applications requiring adaptable material properties. A few such applications are color-changing technologies, “lab on a chip” channels, and self-healing.[1]

One such investigation studies the use of hollow glass fibres imbedded into the laminate of a composite material. These fibres serve to absorb impact energy and can also be filled with uncured resin, hardening agent, and fluorescent dye in the applications of self-healing and damage detection, respectively.[2] Similarly, the curing agent has been stored in these glass fibres with the hardener encased throughout the laminate using microencapsulation techniques.[3] Regardless of cure packaging, this system is limited to composites which are amendable to glass fibre impregnation, and the system is primitive in the fact that it has no controllable branching.

Another area of current research focuses on controllable geometries of vascular systems which ensure accurate patterning and flow but are expensive and time consuming. This

---

[1] David R. Emerson, Krzysztof Cies´licki, Xiaojun Gua, and Robert W. Barbera, "Biomimetic Design of Microfluidic Manifolds Based on a Generalised Murray’S Law" *Lab on a Chip* vol. 6 (2006), p. 447-454.

[2] IP Bond and JWC Pang, "Bleeding Composites- Damage Detection and Self-Repair Using a Biomimetic Approach" *Composites* vol. 36 (2005), p. 183-188.

[3] RS Trask, IP Bond, and GJ Williams, "Bioinspired Self-Healing of Advanced Composite Structures Using Hollow Glass Fibres" *Journal of the Royal Society Interface* vol. 4 (2006), p. 363-371.

work includes photolithographic direct write techniques for 2-dimensional systems.[4] Robotic deposition is used for 3D systems in which a fugitive organic ink is written onto the scaffold structure which is then flooded with epoxy resin. When the epoxy is cured and the ink is removed, it leaves behind the flow channels desired.[4] Channeling has also been accomplished by laser micro-machining into the epoxy system, which requires even greater resources than fugitive ink deposition.[5]

1.2 Natural Vascular Systems

Vascular systems can be seen in many biological forms. Plants, for example, have vascular systems that serve to transfer nutrients from root to leaf. The vascular systems of animals are vast and complicated. They serve as a transport mechanism for liquids and materials, and serve to quickly remove and add resources to the areas of the body which need them. Animals grow to their various sizes due to their vascular networks. A simple diffusive mechanism would not be nearly as efficient at fluid transport and nutrient diffusion over long distances in large bodies. Circulatory systems are the highway of the body, and have served as inspiration for many researchers to find a biomimetic system which can emulate that efficiency.

---

[4] Daniel Therriault, Scott R. White, and Jennifer A. Lewis, "Chaotic Mixing in Three-Dimensional Microvascular Networks Fabricated by Direct-Write Assembly" *Nature* (2003).

[5] Daniel Therriault, Scott R. White, Jennifer A. Lewis, and Robert F. Shepher, "Fugitive Inks for Direct-Write Assembly of Three-Dimensional Microvascular Networks" *Advanced Materials* vol. 17 (2005), p. 395-399.

1.3 Branching Patterns in Nature

Branching patterns which exist in nature provide motivation and a standard to strive toward biomimetic systems in multiple synthesized applications.

1.3.1 Charge-Driven Instabilities

Inspiration can be gained from electrical treeing, a phenomenon which occurs in electrical insulating materials as seen in Figure A. Also known as Lichtenberg figures, these are the cause of the eventual breakdown of a dielectric material. There are two main stages to electrical treeing. The first is the initial "void" formed where there is a region of high electrical stress. The second is the branching structure which is originated at the initial void in the dielectric material. This is propagated by partial charges until the breakdown reaches the electrode. Current can then flow through the dielectric, which is what causes breakdown in electrical insulators used in industry.[6] Current has the ability to flow through this treeing because it has been shown using Raman spectroscopy that the tree structure is comprised of empty channels through the dielectric (such as polyethylene) which may or may not have carbon deposits along the channel walls.[7] This natural phenomenon can be compared to lightning, where charged particles are traveling from one point to another yet want to get away from each other at the same time, creating the branching effect we see.

---

[6] SJ Dodd, "A Deterministic Model for the Growth of Non-Conducting Electrical Tree Structures" *Journal of Physics D: Applied Physics* vol. 36 (2002), p. 129-141.

[7] AS Vaughn, SJ Dodd, and SJ Sutton, "Raman Microprobe Study of Electrical Treeing in Polyethylene" *Journal of Materials Science* vol. 39 (2004), p. 181-191.

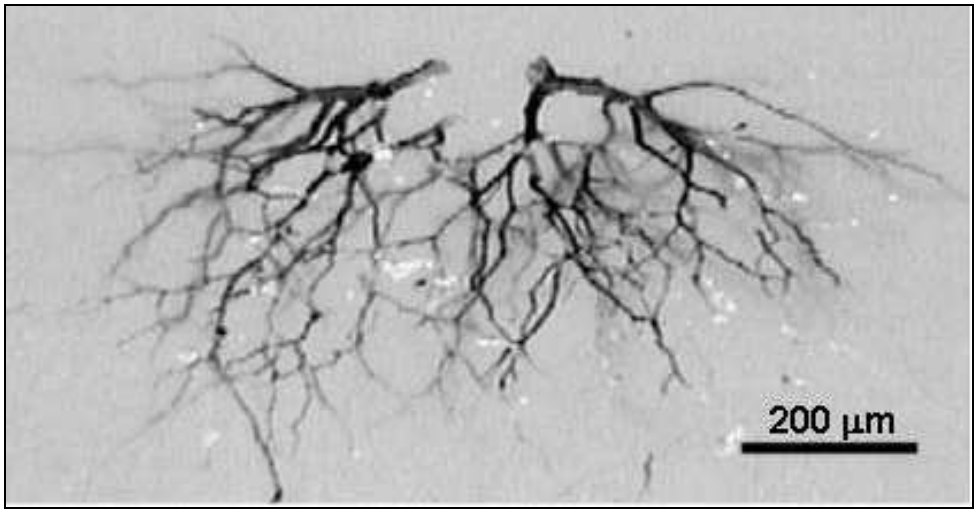

Figure 1: Electrical Treeing in Polypropylene Sample[8]

1.3.2 Viscous Fingering

Employing a different natural phenomenon can create figures known as Saffman-Taylor instabilities, or viscous fingering. Fingering results from the flow of a less viscous fluid through a more-viscous fluid matrix, as seen in Figure 2.

[8] AS Vaughn, et al., *J. Mat Sci*. vol. 39 (2004), p181-191.

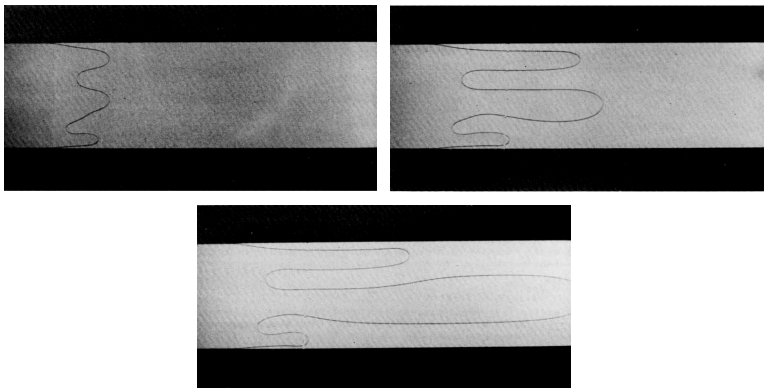

Figure 2: Viscous Fingering Example[9]

The phenomena of viscous fingering is often associated with Hele-Shaw flow, in which the flow domain is confined to a small gap. It has been found experimentally that an initial finger protrudes from the injection site until an instability length scale has been reached. This length scale is particular to the capillary number of the system, but there is experimental evidence of a near-periodic splitting with constant length scales between branches.[10] A capillary number threshold must be crossed in order to obtain fingering. The instability which creates this branching pattern is the basis and starting point of this research project.

1.4 Objective

Applying the basic principles of the branching patterns found in nature, the aim of this thesis work is to combine Saffman-Taylor instability in a two-dimensional Hele-Shaw

[9] Tabeling et al, *J. Fluid Mech* vol. 177 (1987), p. 67-82.

[10] CW Park, and GM Homsy, "The Instability of Long Fingers in Hele-Shaw Flows" *Physics of Fluids* vol. 28 (1985), p. 1583-1585.

flow plane with an applied electrical potential across a dielectric matrix in order to grow and control branching patterns in a curable polymeric system. This is done by first characterizing the growth of a branching pattern created by combining the two natural phenomena, then controlling that growth, and finally, curing the matrix material around the branched structure leaving a hollow cavity. Final work involves the fill and flow of fluid through these cavities.

CHAPTER 2: DIMENSIONLESS ANALYSIS

Categorizing and comparing the different stresses associated with this system allowed for the analysis of various dimensionless numbers. These are helpful when used to explain in a quantitative manner the different flow patterns observed when operating conditions are changed.

2.1 Dimensional Experimental and Material Parameters

The electrohydrodynamic flow in the Hele-Shaw cell can be characterized by the following material and experimental parameters. These can be categorized into flow, interfacial, and electrical parameters as seen in Table 1.

Table 1: Primitive Variables

Category	Experimental Parameters	Symbol
Fluid	Matrix Viscosity	μ_m
	Injection Fluid Viscosity	μ_i
	Interfacial Tension	γ
	Fluid Densities	ρ
Flow	Gap Height	h
	Injection Flow Rate	Q
	Needle Diameter	d
Electrical	Needle Voltage	V
	Distance Between Poles	a
	Dielectric Constant	ε

These parameters can be further consolidated by defining the characteristic flow velocity and electric field. Characteristic flow velocity can be defined either by the diameter of the injection needle or by the height of the flow cell. Since our pattern extends well beyond the tip of the needle, it is reasonable to assume that the height of the Hele-Shaw cell is more influential on the flow pattern than the needle diameter. The two definitions are described in Equations 1 and 2:

$$U \approx \frac{4Q}{\pi h^2} \tag{1}$$

$$E \approx \frac{V}{a} \tag{2}$$

This makes categorization of experimental parameters change slightly, as reflected in Table 2.

Table 2: Condensed Experimental Variables

Category	Experimental Parameters	Symbol
Fluid	Matrix Viscosity	μ_m
	Injection Fluid Viscosity	μ_i
	Interfacial Tension	γ
	Fluid Densities	ρ
Flow	Characteristic Flow Velocity	U
	Needle Diameter	d
Electrical	Characteristic Electrical Field	E
	Dielectric Constant	ε

2.2 Summary of Stresses

The stresses associated with this system can be defined in terms of the experimental parameters described in Table 2. The gap height of the Hele-Shaw flow cell is used as the characteristic length scale for the stress definitions, keeping consistent with the parameter used in defining characteristic flow velocity. It is assumed that this gap height most accurately reflects the diameter of the flow pattern throughout the cell.

Viscous stress compares viscosity of the matrix to the volumetric flow rate and scales accordingly to:

$$\sigma_v = \frac{\mu_m U}{h} \tag{3}$$

Inertial stress is associated with Newton's law of motion and is on the order of:

$$\sigma_i = \rho U^2 \tag{4}$$

Capillary stress is characterized by the interfacial tension between the two fluids. It scales accordingly to:

$$\sigma_c = \frac{\gamma}{h} \tag{5}$$

Electric stress is characterized by the dielectric qualities of the matrix fluid as well as by the strength of the electric field applied to the cell. It is on the order of:

$$\sigma_e = \varepsilon \varepsilon_o E^2 \tag{6}$$

2.3 Dimensionless Numbers

Table 3 contains a summary of the dimensionless numbers which can be used to characterize this system. All are defined in terms of the stresses discussed in section 2.2.

Table 3: Dimensionless Number Analysis

	Viscous stresses	**Inertial stresses**	**Capillary stresses**	**Electrical stresses**
Viscous stresses	$\lambda = \frac{\mu_i}{\mu_m}$	$\mathrm{Re} = \frac{\sigma_i}{\sigma_v} = \frac{\rho U h}{\mu_m}$		$\mathrm{Ga} = \frac{\sigma_e}{\sigma_v} = \frac{\varepsilon\varepsilon_o E^2 h}{\mu_m U}$
Inertial stresses				
Capillary stresses	$\mathrm{Ca} = \frac{\sigma_v}{\sigma_c} = \frac{\mu_m U}{\gamma}$	$\mathrm{We} = \frac{\sigma_i}{\sigma_c} = \frac{\rho U^2 h}{\gamma}$		$\mathrm{Bo} = \frac{\sigma_e}{\sigma_c} = \frac{\varepsilon\varepsilon_o E^2 h}{\gamma}$
Electrical stresses		$\mathrm{Fr} = \frac{\sigma_i}{\sigma_e} = \frac{\rho U^2}{\varepsilon\varepsilon_o E^2}$		

The electrical Bond number (Bo) is the ratio of electrical to capillary stress and is adapted to the system from the conventional Bond number (ratio of gravitational forces to capillary forces).[11] Bo for our purposes measures the importance of electrical forces in comparison to capillary/surface tension forces.

The electrical Galileo number (Ga) is the ratio of electrical to viscous stress, and is also adapted to this system from the conventional Galileo number. The Galileo number is the ratio of gravitational forces to viscous forces. In both the Galileo and Bond numbers, simply substituting electrical field forces for gravitational forces allows for the adaptation

[11] James O. Wilkes, *Fluid Mechanics for Chemical Engineers* 2nd ed., Upper Saddle River, N.J, Prentice Hall PTR, 1999, Print.

of the term to the Hele-Shaw two-dimensional flow system. The electrical Galileo number measures the importance of electrical forces in comparison to viscous forces.

The Weber number (We) is defined as the ratio of inertial forces to capillary forces.

The electrical Froude number (Fr) denotes the ratio of inertial forces to electrical forces. As was defined for Bo and Ga, Fr is adapted from the conventional Froude number[12] which includes gravitational forces rather than electrical.

The Reynolds number (Re) shows the ratio of inertial forces to viscous forces. It provides a value to measure the comparative importance of the two forces during flow. Low Reynolds numbers determine a laminar, or streamlined flow. High Reynolds numbers denote turbulent flow in the system, and the classifications of each flow regime vary depending on the flow geometry.[13] In the Hele-Shaw system, the Reynolds number can be determined using the relation for that of flow through a wide duct, where the width of two parallel plates is much larger than the height between them.

The capillary number (Ca) is defined as the ratio of viscous forces to capillary forces. It takes the viscosity and interfacial tension into account between two immiscible fluids, such as in our oil and water system. Large capillary numbers indicate more temporally

---

[12] Hubert Chanson, *Hydraulics of Open Channel Flow: An Introduction* 2nd ed., Oxford [UK], Elsevier Butterworth Heinemann, 2004, Print.

[13] David R. Lide, ed., *CRC Handbook of Chemistry and Physics*, Internet Version 2007, (87th Edition), <http:/www.hbcpnetbase.com>, Taylor and Francis, Boca Raton, FL, 2007.

stable fingering since it denotes that the interfacial tension between the two fluids has less of an effect.[14]

The viscosity ratio (λ) takes into account the relative viscosities of the injection and matrix fluids. This number is used to characterize the system in reference to both viscosities and can therefore reduce the number of system variables.

2.4 Reduction to Critical Dimensionless Numbers

The overall cell is relatively small in size, flow occurs through a narrow gap, and viscous materials are used. Therefore, calculating We, Fr, and Re shows that inertial effects are unimportant in this system. For example, consider a typical system of 17 kV applied to a 12,500 cSt silicone oil matrix with no surfactant and an injection rate of 0.2 mL/min. Under these conditions, We= 8.5×10^{-4}, Fr= 4.6×10^{-6}, and Re= 4.2×10^{-4}. All three of these dimensionless values are well below unity, indicating that inertial stresses are overcome by capillary, electrical, and viscous stresses, respectively. Therefore, We, Fr, and Re can be ignored in the initial analysis. In order to further reduce the dimensionless numbers used to characterize the flow, it should be noted that Ga is the ratio of Bo to Ca. This leaves us with three main parameters of λ, Ca, and Ga.

[14] P Tabeling, G Zocchi, and A Libchaber, "An Experimental Study of the Saffman-Taylor Instability" *Journal of Fluid Mechanics* (1986), p. 67-82.

2.5 Qualitative Terminology

Due to the preliminary stage of this research, a large portion of the results are shown in a qualitative manner. Photographs and videos of flow studies were used to determine the effects of process parameters, and were compared side by side. The results were also used to determine the accuracy of pattern predictions made with the dimensionless analysis. This section defines the qualitative terms that are used to describe the visual results of each study.

Degree of branching: The degree of branching is defined by the total amount of branches that are created.

Length scale between branches: The length scale between branches is the distance along a main branch between the branches that have been created off of it. If branches are created closer together, the length scale between them is smaller, and vice versa.

Density of branches: Density of branches describes the amount of branching that has occurred. This describes if a few small branches have been created, or if a large network of them are spread throughout the sample.

Droplet formation: Droplet formation describes when a part of the branch breaks off and becomes an electrically neutral water droplet that is completed separated from the rest of the channel by the matrix.

Pooling: Pooling is a phenomena that occurs mainly at high injection flow rates. This term describes when a branched channel begins to grow and form a reservoir within the matrix.

Branch relaxation: Branch relaxation is used to describe when the injected material becomes electrically neutral and no longer exhibits sharply defined branches. There is a softening of the channel profile when this occurs.

CHAPTER 3: EXPERIMENTS WITH SILICONE OIL MATRIX

3.1 Materials

3.1.1 Silicone Oils

The matrix material used for the experimental setup is silicone oil in a variety of viscosities. The viscosities used extensively were 1,000 cSt (Shin Etsu Chemical Company Lot Number 705366), 12,500 cSt (www.thechemistrystore.com Product Number 82024-1), and 100,000 cSt (Shin Etsu Chemical Company Lot Number 701424) oils. These are electrical insulators with a dielectric constant of 2.4.

3.1.2 Surfactants

While multiple surfactants were tested, the most success was found with Dow Corning (Midland, MI) 190-fluid. This is mixed directly with the silicone oil and serves to reduce the interfacial tension between the matrix and injection fluids.

3.2 Equipment

The Hele-Shaw flow cell used in this experiment is pictured in Figure 3. The cell used for the silicone oil experiments is made from two 0.25” polycarbonate pieces. The two are screwed together with 21 gauge needle spacers to ensure equal pressure and spacing throughout the cell. The injection needle is also 21 gauge, or 0.8 mm in diameter. The positive lead is attached to the injection needle, which positively charges the water as it is

flowing through. The ground lead is attached to a strip of copper tape at the end of the Hele-Shaw cell. The U-shaped white gasket is made from a 1/16th inch-thick white closed-cell FDA polyethylene foam.

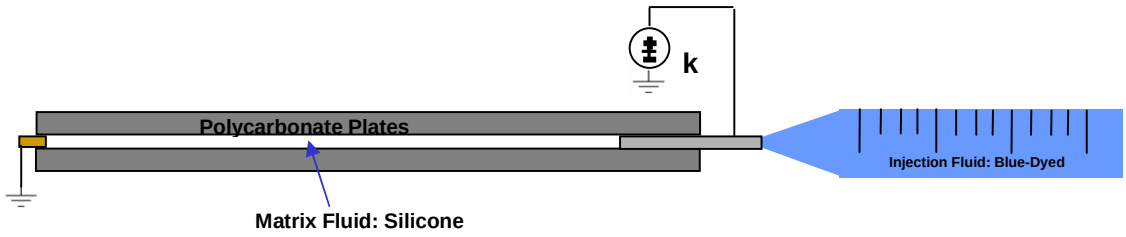

Figure 3: Schematic of Hele-Shaw 2D Flow Cell

Figure 4 is a photograph of the experimental setup. This is the top view of the diagram from Figure 3. Seen at the far right of Figure 4 is the syringe pump used to control the volumetric flow rate of the injection material. The cell is electrically insulated from the countertop and syringe pump by silicone rubber pieces. Also note the timer in the bottom of the frame. This is used to time the studies and determine volume of fluid injected.

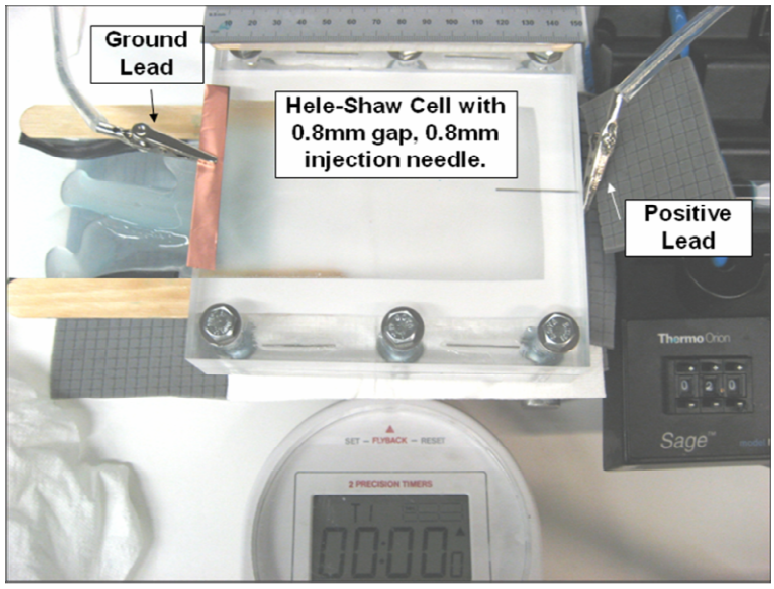

Figure 4: Photograph of Hele-Shaw 2D Flow Cell

3.3 Experimental Procedure and Considerations

The general procedure for completing this experimental run is as follows:

I. Collect 20g of matrix fluid and 5mL of injection fluid
    i. De-gas matrix fluid in a vacuum oven to eliminate air bubbles

II. Prepare Hele-Shaw Cell
    i. Attach copper tape at end of top plate to act as ground
    ii. Prime injection needle with fluid
    iii. Fill area inside gasket with matrix fluid, close top, and tighten

III. Attach positive lead to needle and ground lead to copper tape

IV. Use high-voltage source to obtain the desired potential across the cell

V. Start timer and injection

VI. Take pictures at a regular interval throughout the injection

VII. Remove voltage when water reaches the ground plane

Variations to the general procedure have been done for point charge testing in an effort to control the flow of the injection material, as will be described in the results section of this report.

The original baseline conditions of this experiment were to inject water into a 12,500 cSt silicone oil matrix at a volumetric flow rate of 0.2 mL/min through a 21 gauge injection needle and spacers with 17 kV of applied potential and 0 wt% surfactant. As studies progressed and data was analyzed to determine the various effects of process parameters, the baseline conditions changed to an electrical potential of 17 kV, flow rate of 0.2 mL/min, and 0.5 wt% surfactant for a 100,000 cSt silicone oil cell and 2.0 wt% surfactant for a 12,500 cSt silicone oil cell. As electrical insulation improved by adding sheet glass and silicone rubber in the setup, the baseline applied voltage increased to 35kV.

Tables 4 and 5 show the testing matrices used to organize the trends found in the results of this experiment in terms of λ, Bo, and Ca. These matrices were also used to explain the qualitative results in terms of quantifiable values. Select results from these experiments will be presented in the Results section of this chapter.

Table 4: Dimensionless Analysis for Silicone Oil Experiments

Voltage (V)	Surfactant	μm (Pa-s)	μi (Pa-s)	Q (ml/min)	U (m/s)	λ	Bo	Ca
0	0	12.5	0.001	0.2	6.6E-03	8.0E-05	0.0E+00	2.0E+00
13000	0.5 190-fluid	100	0.001	0.2	6.6E-03	1.0E-05	4.1E+02	6.0E+01
13000	1 190-fluid	12.5	0.001	0.2	6.6E-03	8.0E-05	4.5E+02	8.3E+00
13000	2 190-fluid	12.5	0.001	0.2	6.6E-03	8.0E-05	5.0E+02	9.2E+00
17000	0	12.5	0.001	0.02	6.6E-04	8.0E-05	1.8E+02	2.0E-01
17000	0	0.001	1	0.2	6.6E-03	1.0E+03	1.8E+02	1.6E-04
17000	0	1	0.001	0.2	6.6E-03	1.0E-03	1.8E+02	1.6E-01
17000	0	12.5	0.001	0.2	6.6E-03	8.0E-05	1.8E+02	2.0E+00
17000	0.5 190-fluid	12.5	0.001	0.2	6.6E-03	8.0E-05	7.0E+02	7.5E+00
17000	1 190-fluid	12.5	0.001	0.2	6.6E-03	8.0E-05	7.7E+02	8.3E+00
17000	1 surfynol	12.5	0.001	0.2	6.6E-03	8.0E-05	7.7E+02	8.3E+00
17000	2 190-fluid	12.5	0.001	0.2	6.6E-03	8.0E-05	8.5E+02	9.2E+00
17000	3 190-fluid	12.5	0.001	0.2	6.6E-03	8.0E-05	8.5E+02	9.2E+00
17000	0	100	0.001	0.2	6.6E-03	1.0E-05	1.8E+02	1.6E+01
17000	0	1	0.001	2	6.6E-02	1.0E-03	1.8E+02	1.6E+00
17000	0	12.5	0.001	2	6.6E-02	8.0E-05	1.8E+02	2.0E+01
17000	2 190-fluid	12.5	0.001	2	6.6E-02	8.0E-05	8.5E+02	9.2E+01
17000	3 190-fluid	12.5	0.001	2	6.6E-02	8.0E-05	8.5E+02	9.2E+01
17000	0	100	0.001	2	6.6E-02	1.0E-05	1.8E+02	1.6E+02
17000	0.5 190-fluid	100	0.001	2	6.6E-02	1.0E-05	7.0E+02	6.0E+02
17000	2 190-fluid	100	0.001	2	6.6E-02	1.0E-05	8.5E+02	7.4E+02
17000	0	12.5	0.001	10	3.3E-01	8.0E-05	1.8E+02	1.0E+02
17000	0	12.5	0.001	20	6.6E-01	8.0E-05	1.8E+02	2.0E+02
27000	0.5 190-fluid	100	0.001	0.2	6.6E-03	1.0E-05	1.8E+03	6.0E+01
27000	0.5 190-fluid	100	0.001	0.2	6.6E-03	1.0E-05	1.8E+03	6.0E+01
27000	0.5 190-fluid	100	0.001	2	6.6E-02	1.0E-05	1.8E+03	6.0E+02
35000	0.5 190-fluid	100	0.001	0.2	6.6E-03	1.0E-05	3.0E+03	6.0E+01

Table 5: Dimensionless Analysis of Curable Pre-Polymer Experiments

Voltage (V)	wt% MFA	μm (Pa-s)	μi (Pa-s)	Q (ml/min)	U (m/s)	λ	Bo	Ca
0	31	100	0.001	0.2	6.6E-03	1.0E-05	0.0E+00	6.6E+01
15	31	100	0.001	0.2	6.6E-03	1.0E-05	6.0E-04	6.6E+01
30	31	100	0.001	0.2	6.6E-03	1.0E-05	2.4E-03	6.6E+01
45	31	100	0.001	0.02	6.6E-04	1.0E-05	5.4E-03	6.6E+00
45	31	100	0.001	0.2	6.6E-03	1.0E-05	5.4E-03	6.6E+01
45	31	100	0.001	2	6.6E-02	1.0E-05	5.4E-03	6.6E+02
45	40.5	50	0.001	0.2	6.6E-03	2.0E-05	5.4E-03	3.3E+01
45	62.2	10	0.001	0.2	6.6E-03	1.0E-04	5.4E-03	6.6E+00
45	93.3	1	0.001	0.2	6.6E-03	1.0E-03	5.4E-03	6.6E-01
45	100	0.5	0.001	0.2	6.6E-03	2.0E-03	5.4E-03	3.3E-01
60	31	100	0.001	0.2	6.6E-03	1.0E-05	9.6E-03	6.6E+01

3.4 Characterization

3.4.1 Rheometry

The TA Instruments Advanced Rheometer Series was used to catalog the viscosity dependence of the vinyl ester system in terms of styrene composition. This was completed systematically by following the TA Instruments supplied rheology instructions. Instrument used was the AR2000 with 40 mm parallel plate geometry with 1 mm gap and accompanying software of Rheology Advantage 4.0.

3.4.2 Electrical Conductivity

The electrical conductivity of the materials tested in this study is assessed by the absence of resistivity. This was accomplished with the use of a multimeter set to the ohmmeter function. High resistivity readings ensured near-dielectric conditions for matrix materials, where low resistivity readings indicated conductive properties of the material.

CHAPTER 4: SILICONE OIL MATRIX RESULTS

All preliminary proof of concept experiments were completed by injecting water into a silicone oil matrix. The process conditions of matrix viscosity, surfactant addition, applied voltage, and injection flow rate were systematically studied. Qualitative results were obtained in this study in order to determine the process effects of the dimensionless terms, which are compared to the final branching structures.

4.1 Effect of Viscosity Ratio

The effect of viscosity ratio was systematically studied by varying the injection and matrix materials of the Hele-Shaw flow. The top left photo in Figure 5 shows 1,000 cSt silicone oil injected into water, the top right photo shows water injected into 1,000 cSt silicone oil, the bottom left shows water injected into 12,500 cSt silicone oil, and the bottom right shows water injected into 100,000 cSt silicone oil matrix. All four injections were completed with 0% surfactant added to the matrix material and 17 kV applied electricity.

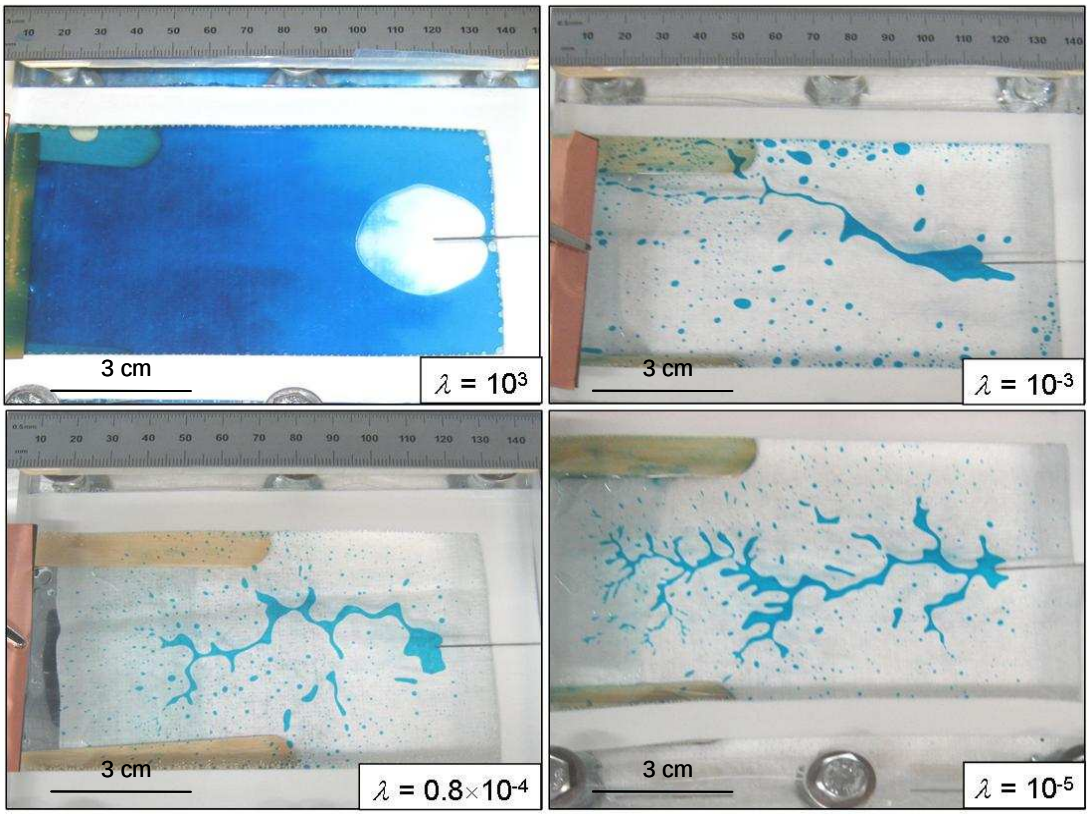

Figure 5: Viscosity Ratio Study Results

Qualitatively, the degree of branching increases with decreasing viscosity ratio. The variance ranges from the highest viscosity ratio producing a nearly perfect circle to the lowest viscosity ratio having a small length scale between branches. The other two viscosity ratios demonstrate appropriate intermediate length scales between these extremes.

Table 6: Viscosity Ratio Study Dimensionless Analysis

λ	Bo	Ca
1.0E+03	1.8E+02	1.6E-04
1.0E-03	1.8E+02	1.6E-01
8.0E-05	1.8E+02	2.0E+00
1.0E-05	1.8E+02	1.6E+01

Note in Table 6 that decreasing the viscosity ratio increases the capillary number while the Bond number remains constant. The Bond number is constant because voltage and surfactant concentration are kept constant in this series of experiments.

The increasing viscosity ratio also has an effect on the droplet formation. As the ratio decreases, droplets become visibly smaller. There is also a decrease in the frequency of droplet formation. This is due to the increasing capillary number of the system with decreasing viscosity ratio. Large capillary numbers show that viscous forces are overtaking capillary forces, and the branches of the system are more stable as a result of the decreasing importance of interfacial tension between the fluids.

Capillary numbers are evaluated on an order of magnitude throughout this entire scope of work, as the exact interfacial tension between silicone oil and water and between vinyl ester and water is not known.

The values used in the dimensionless analysis were estimated from literature values of interfacial tension of silicone oil and water with a varying polyether surfactant

concentration.[15] Interfacial tension is proven to drop as surfactant content increases in similar material systems as those used in this work The surfactant used in the silicone oil study is Dow 190-fluid, and the MFA used in the vinyl ester study (Chapter 6.2) acts as a natural surfactant.. To apply the principal of increasing surfactant to this study, it is assumed that interfacial tension is independent of oil molecular weight and therefore the same trend can be used. Table 7 shows the interfacial tensions assumed for each surfactant wt% used in this study that have been adopted from the literature values.

Table 7: Estimated Interfacial Tension Values

Material	γ (dynes/cm)
Silicone Oil 0.0 wt% Surfactant	41.5
Silicone Oil 0.5 wt % Surfactant	11.0
Silicone Oil 1.0 wt% Surfactant	10.0
Silicone Oil 2.0 wt% Surfactant	9.0
Vinyl Ester 31 wt% MFA	10.0

4.2 Effect of Surfactant

The effect of surfactant was studied by maintaining experimental conditions in the cell while only varying surfactant weight per cent based on the matrix material. The first was done in a viscous environment of 100,000 cSt silicone oil with a volumetric flow rate of 2 mL/min, as seen in Figure 6. The surfactant used was Dow-190 fluid and the applied potential was 17 kV.

[15] AG Kanellopoulos and MJ Owen, "The Adsorption of Polydimethylsiloxane Polyether ABA Block Copolymers At the Water/Air and Water/Silicone Fluid Interface" *Journal of Colloid and Interface Science* vol. 35 (1970), p. 120-125.

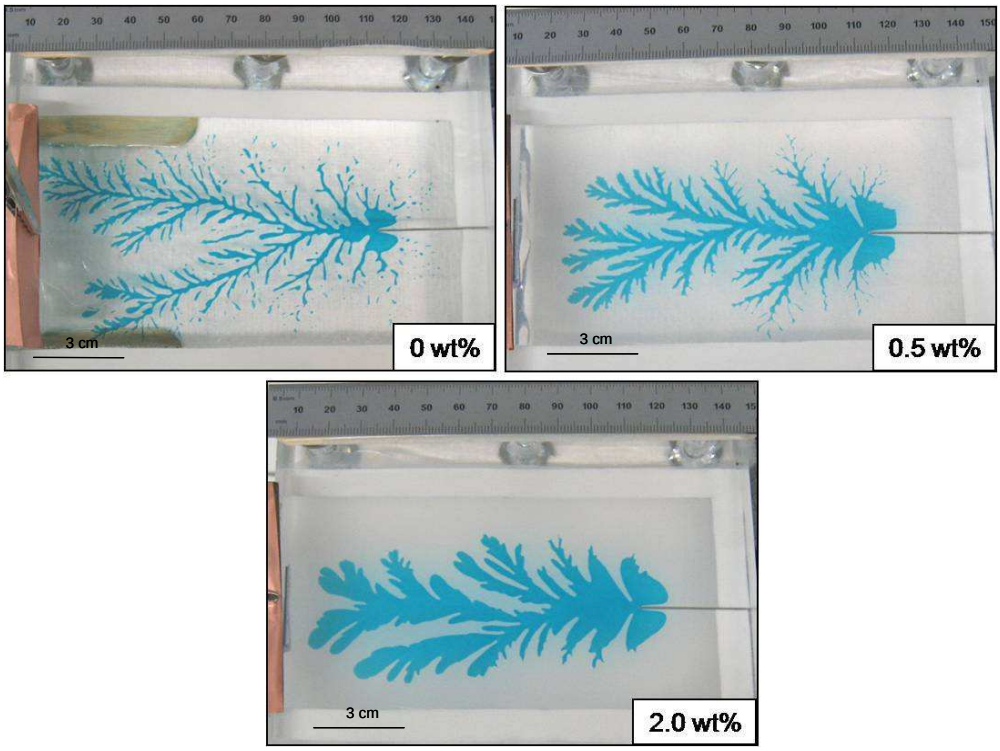

Figure 6: High Viscosity Surfactant Study Results

The interfacial tension is visibly lessened with increasing surfactant concentration. This is seen by the decrease in droplet formation from the branching structures as well as in relaxation of the branches themselves. For the purposes of this study, the optimum surfactant concentration for a 100,000 cSt matrix system is 0.5wt% Dow Corning 190-fluid, which created an intermediate structure with severely decreased amount of droplets yet not much branch relaxation.

Table 8: High Viscosity Surfactant Study Dimensionless Analysis

Surfactant	Bo	Ca
0	1.8E+02	1.6E+02
0.5 190-fluid	7.0E+02	6.0E+02
2 190-fluid	8.5E+02	7.4E+02

While the bond and capillary numbers changed slightly in this experiment, they stayed on the same order of magnitude throughout all process conditions. With the data displayed in Table 8, it can be safely assumed that all qualititative observations were caused by the addition of varying surfactant concentrations.

This study was repeated with a 12,500 cSt silicone oil matrix and lower flow rate at 0.2 mL/min. The results are shown in Figure 7. 17 kV of potential was applied for all runs, and the surfactant used was Dow-190 fluid.

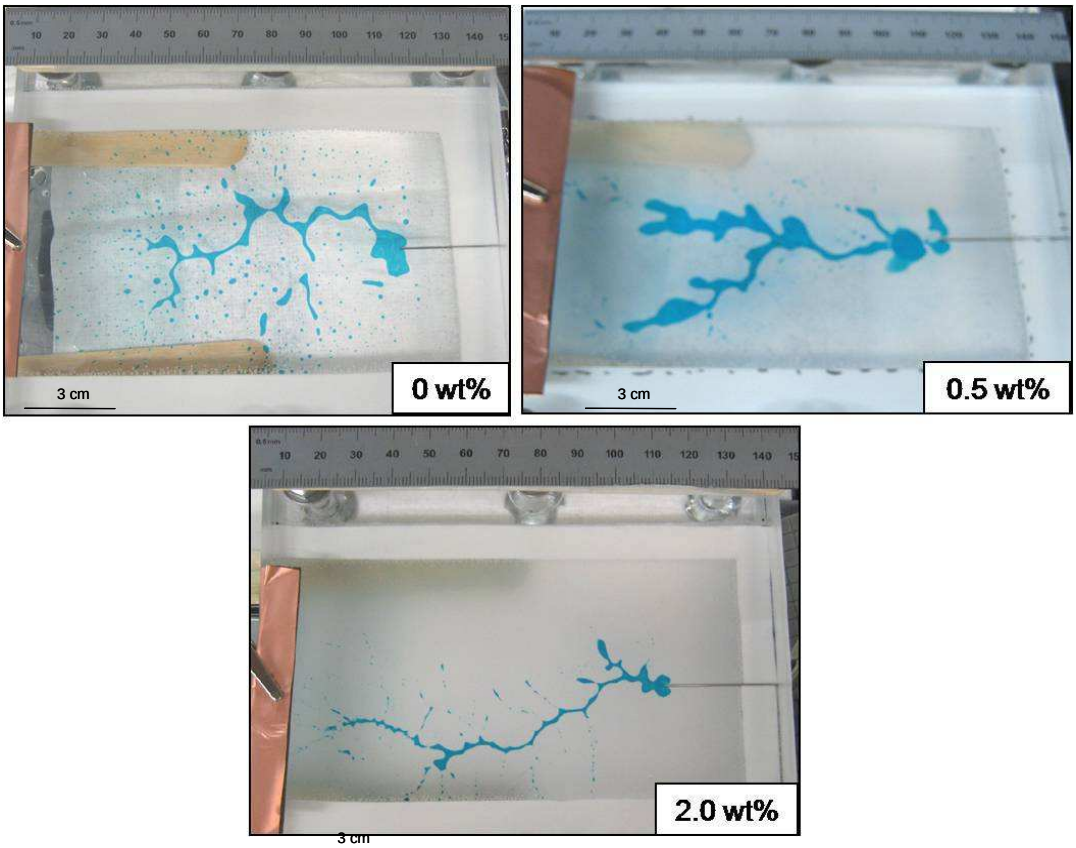

Figure 7: Low Viscosity Surfactant Study Results

As in Figure 6, a decrease in droplet size and formation in occurrence with increasing surfactant concentration in the matrix fluid is seen in Figure 7. For this system, we found the optimum concentration to be 2 wt% Dow Corning 190-fluid surfactant. A systematic determination of interfacial tension between the two fluids will clarify the effect on Ca and will quantify the benefit that surfactant addition has on the system. The estimated dimensionless analysis is shown in Table 9.

Table 9: Low Viscosity Surfactant Study Dimensionless Analysis

Surfactant	Bo	Ca
0	1.8E+02	2.0E+00
0.5 190-fluid	7.0E+02	7.5E+00
2 190-fluid	8.5E+02	9.2E+00

Also following the results of the surfactant study, the Bo and Ca stay on the same order of magnitude across all process conditions that were studied. The results obtained were due to the addition of surfactant.

4.3 Effect of Voltage

The effect of voltage was studied in two ways. The first systematic study determined the value of applying potential across the cell. The second study used placement of electrical charges to direct flow patterns.

4.3.1 Effect of Increasing Electric Field Strength

Systematically increasing electric potential to the system was used to study the effect of electrical stresses on the branching structures. The matrix had a viscosity of 100,000 cSt with 0.5 wt% Dow-190 fluid surfactant. The injection flow rate remained constant at 0.2 mL/min, as voltage was increased systematically from 0 kV to 35 kV. The results are shown in Figure 8.

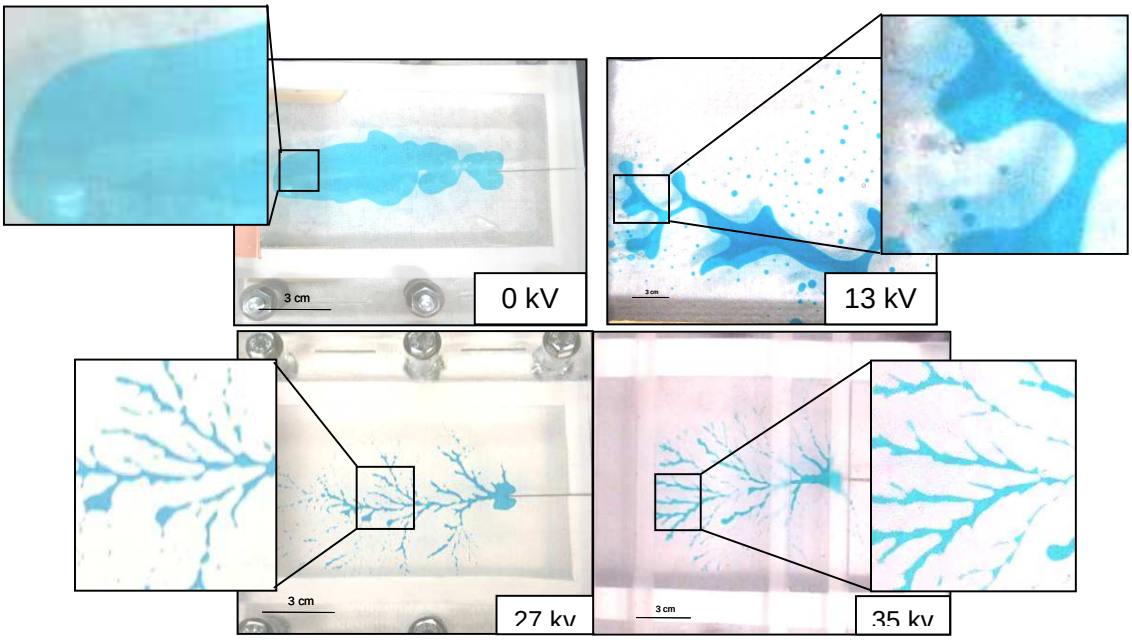

Figure 8: Voltage Study Results

Figure 8 qualitatively shows that increasing the applied voltage to the system will increase the degree of branching, and decrease the length scale between branches. The results obtained vary from a simple viscous fingering example to a branching structure that is highly fractal. Table 10 is used to compare the dimensionless terms to the qualitative results from the study.

Table 10: Voltage Study Dimensionless Analysis

Voltage (V)	Bo	Ca
0	0.0E+00	2.0E+00
13000	4.1E+02	6.0E+01
27000	1.8E+03	6.0E+01
35000	3.0E+03	6.0E+01

Table 10 shows the accompanying dimensionless analysis for the voltage study. While Ca remains constant, Bo increases. This shows the increasing effect that electrical stresses are having on the system and the beneficial effect that it has on the branching structure.

4.3.2 Effect of Directional Electric Fields

Applied potential can also be used to direct the flow of the system. Control of the system growth was tested through the use of point charges located strategically along the edge of and inserted into the silicone oil cell. Results can be seen in Figures 9 and 10. For both runs, water was injected at 0.2 mL/min into a 100,000 cSt silicone oil matrix, with 0.5 wt% Dow-190 fluid surfactant.

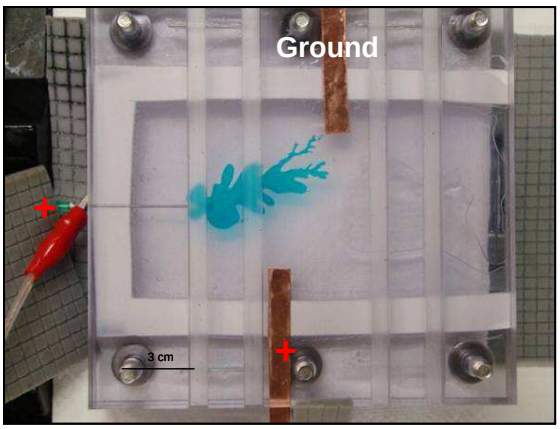

Figure 9: Directional Study Results – Left

Figure 9 shows the first run where a positive lead was inserted on the bottom of the cell, and 15 kV of potential was applied to both the positive lead and the injection needle. A definite trend away from the positive lead and towards ground was observed.

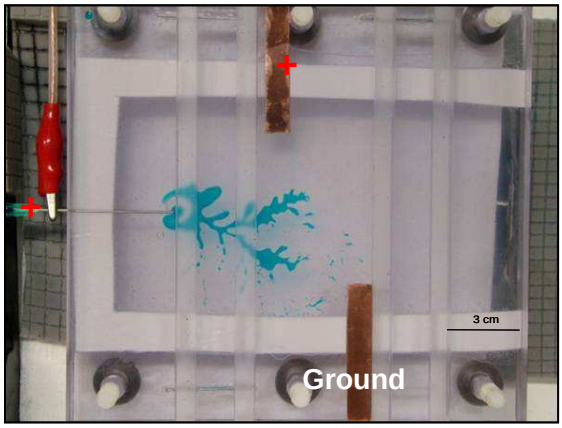

Figure 10: Directional Study Results – Right

In order to prove the effectiveness of this technique, the location of positive and ground leads were reversed as seen in Figure 10. In this run, 20 kV was applied to the injection needle and the positive lead in an attempt to increase branching of the system. Again, a trend away from the positive lead and towards ground was observed. The branching increased with the increased applied voltage, as expected.

4.4 Effect of Flow Rate

The effect of flow rate on the branching structure was observed by systematically increasing volumetric flow rate of the injection material while maintaining all other experimental conditions; including a 17 kV applied potential, 12,500 cSt silicone oil matrix, and no surfactant content. Results are shown in Figure 11.

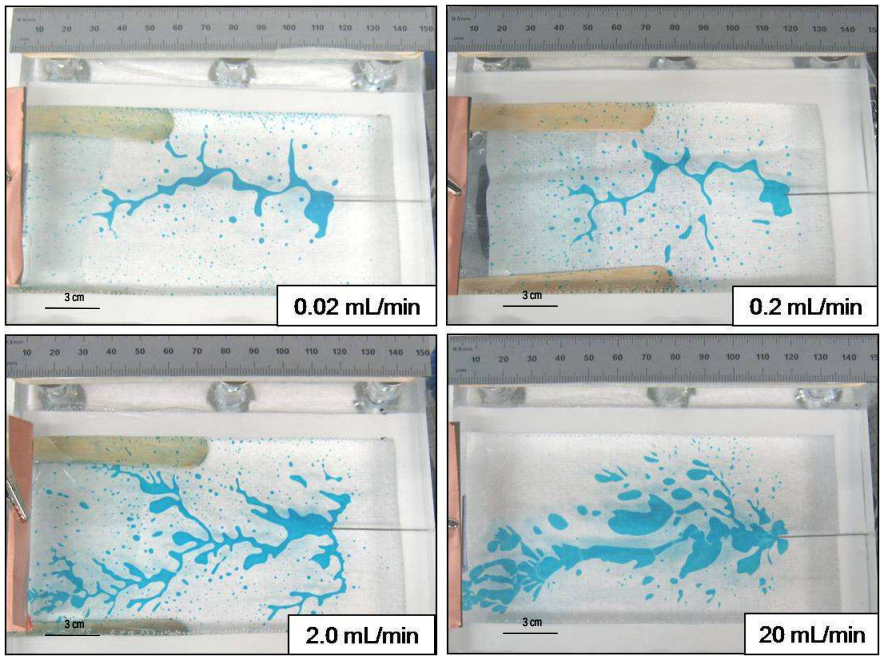

Figure 11: Flow Rate Study Results

Qualitative inspection of Figure 11 shows an increase in "pooling" throughout the branching structure in response to an increase in volumetric flow rate. This is consistent with theories in fluid dynamics. Bernoulli's principle shows that an incompressible fluid will flow from an area of higher pressure to an area of lower pressure.[16] The principle also states that fluid will have a greater speed going from an area of higher pressure to an area of lower pressure, and a lesser speed in the opposite direction. As the injected volumetric flow rate is increased, a greater volume of material is forcing its way through the same size channel, since the injection needle diameter has not changed. This increases the pressure exerted on the walls of the channel, and forces them outward into the pools as seen in the above figures. Following Bernoulli's principle, as the fluid travels from an

[16] James Welty and Charles E. Wicks, *Fundamentals of Momentum, Heat, and Mass Transfer*, New York, Wiley, 2001, Print.

area of high pressure to one of low pressure, the velocity decreases, therefore allowing material to accumulate. The dimensionless analysis for the flow study is summarized in Table 11.

Table 11: Flow Rate Study Dimensionless Analysis

Q (ml/min)	Bo	Ca
0.02	1.8E+02	2.0E-01
0.2	1.8E+02	2.0E+00
2	1.8E+02	2.0E+01
20	1.8E+02	2.0E+02

Table 11 shows that the capillary number increases linearly with increasing volumetric flow rate. An increased Ca is associated with more stable fingering patterns, which will show an increase in Saffman-Taylor instabilities. This effect is seen in Figure 11, which shows that the interfacial interactions between the two fluids are becoming less important with increasing flow rate. This will become more pronounced when the exact interfacial tension between the two materials is studied and taken into account in the dimensionless terms. These effects are studied in an isolated manner by keeping the Bond number constant, as shown in Table 11.

4.5 Silicone Oil Matrix Learnings- Effects of Process Conditions

The overall goal of the thesis project is to consistently direct the growth of a finely branched structure in a curable matrix medium. The preliminary studies performed with a silicone oil matrix were conducted in order to determine the effects of each processing

condition. These studies were also used to test the reliability of the dimensionless analysis in predicting the flow patterns of the injected material.

Qualitatively, the degree of branching increases with decreasing viscosity ratio. As this viscosity ratio decreases, the capillary number also increases. Even though the Bond number is consistent, the effect of the viscous stress becomes more prominent, resulting in the high degree of branching and decrease in droplet formation. The desired process condition to ensure this behavior is a high matrix material viscosity.

With increasing surfactant content in the matrix, the interfacial tension between these immiscible fluids appears to decrease, droplet formation decreases, and branching in the system decreases to an extent. These observations are paired with dimensionless numbers which are not affected by an order of magnitude change. There is a slight increase in both Bond and capillary numbers with increasing surfactant concentration. When Ca reaches a value larger than Bo, the length scale between branches gets too large. The desired process condition to ensure the highly branched behavior without droplet formation is some addition of surfactant to decrease the interfacial tension between the phases. However, excess surfactant must be avoided to ensure a high degree of branching.

Increasing applied voltage across the cell results in a decreased length scale between branches. It is hypothesized that the larger charge carried by the water causes smaller changes in flow pattern to result in charge-driven fractals. As voltage is increased, the Bond number increases even while the capillary number remains constant, showing an

increase in electrical stress on the system. The desired process condition to ensure small length scales between branches is a high voltage applied across the cell.

The use of positive leads is encouraged in directing the flow of the branching pattern. It has been proven experimentally that moving the ground has limited success in directing the path of the channels. However, including multiple positive leads which the positively charged conductive material wants to avoid has effectively driven the entire branching system in one direction or another, even at low applied voltages.

Increasing flow rate increases the frequency and severity of pooling in the branches. Very similarly to the surfactant study, as injection volumetric flow rate was increased, the capillary number increased while the Bond remained constant. Pooling increases with each increase in flow rate, and is unacceptable at the point where Ca is greater than Bo.

When the processing conditions of matrix viscosity, surfactant concentration, voltage, and injection flow rate have been tuned to the system, it is possible to grow an intricately branching channeled structure with the properties desired for flow applications. These conditions must be tuned so that the electric stress is greater than the viscous stress, which in turn is greater than the capillary stress on the system. Simultaneously, the viscosity ratio must be minimized. These stresses can be summarized using the dimensionless analysis on the system. A large Bond number greater than the capillary number, which in turn is at least greater than unity will consistently predict well defined

branching structures in any variety of matrix materials. Figure 12 shows an example of a finely tuned system that has been achieved.

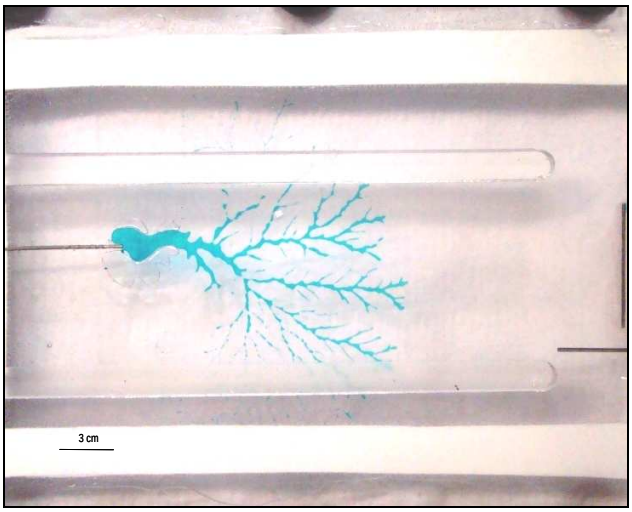

Figure 12: Well Defined Branched Structure in Silicone Oil Matrix

Note in Figure 12 that this structure has many of the qualities that are desired for end-result application. The channels are self-propagating, there are various sizes of branch diameters and lengths, and different structures are achievable with the use of positive lead placement. Processing conditions for Figure 12 were to inject water into a 100,000 cSt silicone oil system with 0.5 wt% 190-fluid at a volumetric flow rate of 0.2 mL/min and an applied potential of 35 kV. The injection was turned off midway through the experiment, and branching occurred only through electrical stresses for the remainder of the cell. Bo is 3.0 x 10^3 and Ca is 6.0, which follows the recommended dimensionless values that were developed as the outcome of this study.

CHAPTER 5: PRELIMINARY CURED SYSTEMS

Two pre-polymer materials were used in preliminary cure studies of these branching systems. Both matrices were cured using an in-situ method, where a UV light was applied to the system as the branching structure was formed. Both a flexible material, Ebecryl, and a rigid material, Vinyl Ester, were tested.

5.1 Materials

5.1.1 Ebecryl 230

Ebecryl 230 becomes a flexible polyurethane material once it has been cured. The un-cured resin has a viscosity of approximately 30,000 cSt and is electrically insulating. The system is UV cured by adding 1.5 wt% Irgacure photoinitiator. Curing the system is achieved by applying UV light for two minutes and is postcured by heating to 80^{o}C and again applying UV light.

5.1.2 Irgacure

Irgacure 184 is a commercially available photoinitiator produced by Ciba Specialty Chemicals. The chemical structure for this commercial product is 1-Hydroxyl-cyclohexyl-phenyl-ketone, and absorbs UV light in the 246-333 nm range.[17]

5.1.3 CN-151

The rigid polymer used in this study is a vinyl ester resin, CN-151 (Sartomer) which is a bisphenol A epoxy methacrylate oligomer.

5.1.4 Styrene

Styrene, a reactive monomer, is used as the diluent for this system which allows for the tailoring of viscosity of the system.

5.1.5 Camphorquinone

Camphorquinone, or $C_{10}H_{14}O_{2,}$ is a photoinitiator for polymerization commonly used with blue light or UV light. It is added to the pre-polymer in the same weight ratio as tetramethylaniline to initiate cure.

5.1.6 Tetramethylaniline

N,N,3-5-tetramethylaniline, or $(CH_3)_2C_6H_3N(CH_3)_2$, is a photoreducer used in concert with camphorquinone[18] for cure of a vinyl ester or other pre-polymer.

---

[17] *Ciba Specialty Chemicals*, Web, 20 Oct. 2009, <http://www.ciba.com>.

[18] *Sigma Aldrich*, Web, 20 Oct. 2009, <http://www.sigmaaldrich.com>.

5.2 Cured Ebecryl Matrix Structures

The results of an Ebecryl cure study are shown in Figure 13. The experimental conditions which resulted in this figure were to apply a 13 kV electrical potential across the Hele-Shaw cell and inject water into the cell at a flow rate of 0.2 mL/min. The resulting structure is flexible with a consistent thin layer formed on either side of the branches, making them complete channels. Due to the low viscosity of the material as well as the relatively low voltage, the degree of branching is low for this system.

Figure 13: Cured Ebecryl-230 Branching Structure

The dimensionless analysis for this experiment yields a viscosity ratio of 3.6×10^{-5}, a Bond number of 1.08×10^{2}, and a capillary number of 4.6. This is a well-defined system, with a high degree of branching. The qualitative results shown in Figure 13 are reflected by the high Bond number, which is higher than the capillary number, which is higher

than unity. Ebecryl also creates a flexible polymer, with branched channels which bend and flex along with the material.

5.3 Cured Vinyl Ester/Styrene Matrix Structures

Vinyl ester is a rigid polymer once cured, and has a tailorable viscosity when a reactive monomer, styrene, is added. It is also electrically insulating. Formulation of a UV-curable system begins with the tailored viscosity of CN-151 vinyl ester resin and styrene. Using a TA-Instruments Rheometer, the viscosity of the system as a function of styrene content was measured and is summarized in Figure 14.

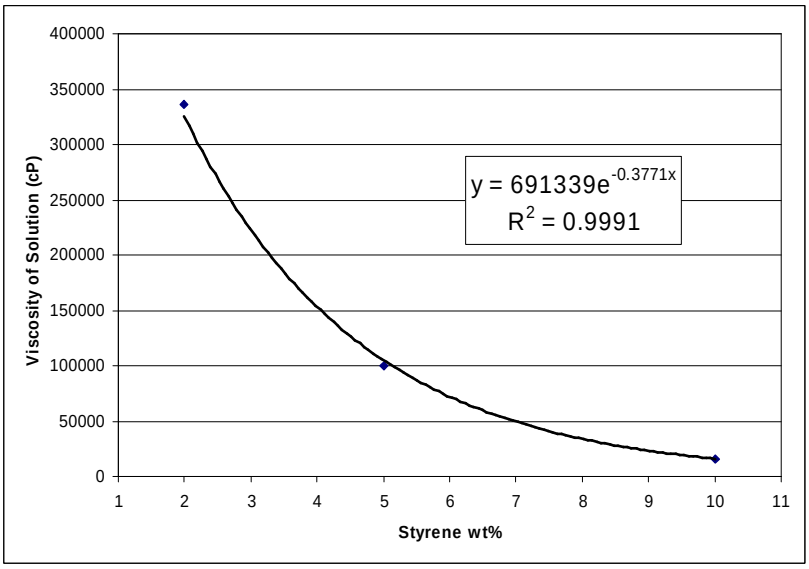

Figure 14: CN-151/Styrene Viscosity as a function of styrene content at 25°C

Since the initial silicone oil experiments were conducted mainly at 12,500 cSt and 100,000 cSt, these system conditions must be recreated in order to fabricate pre-polymer

results consistent with those already obtained in silicone oil. The two units in Equation 7 are easily converted.

$$cSt = \frac{cP}{S.G.} \tag{7}$$

The specific gravity of CN-151 is 1.14 and since the system has a majority concentration of vinyl ester (less than 10% styrene), it can be assumed that the total system S.G. is approximately 1.14.

The desired styrene content can be found by solving the equation given for styrene wt % (the x-axis in the figure). The result is given by Equation 8.

$$wt\% = -2.6518 \ln\left(\frac{SG * cSt}{691339}\right) \tag{8}$$

A 12,500 cSt system of vinyl ester requires 10.29 wt% styrene in the system. For a 100,000 cSt system, 4.78 wt% styrene is required. 0.5 wt% of camphorquinone is then added. This photoinitiator creates the free radicals to enable the vinyl ester system to polymerize structure. 0.5 wt% of tetramethylaniline is also added, which acts as the photoreducer and donates the electron or proton required to induce the initiator into creating free radicals.[19] The system is cured by applying UV light for two minutes. Post cure involves heating the material to 70°C and again applying UV light.

---

[13] F Cardona, D Rogers, S Davey, and G Van Erp, "Investigation of the Effect of Styrene Content on the Ultimate Curing of Vinylester Resins by TGA-FTIR" *Journal of Composite Materials* vol. 41 (2006), p. 137-152.

The results of one vinyl ester cure study can be found in Figure 15. The experimental conditions for this sample included a 35 kV voltage applied to the cell and water injected at a flow rate of 0.2 mL/min. The vinyl ester has 5 wt% styrene, or a viscosity of 100,000 cSt and 0.67 wt% each of camphorquinone and tetramethylaniline were added to initiate the UV polymerization.

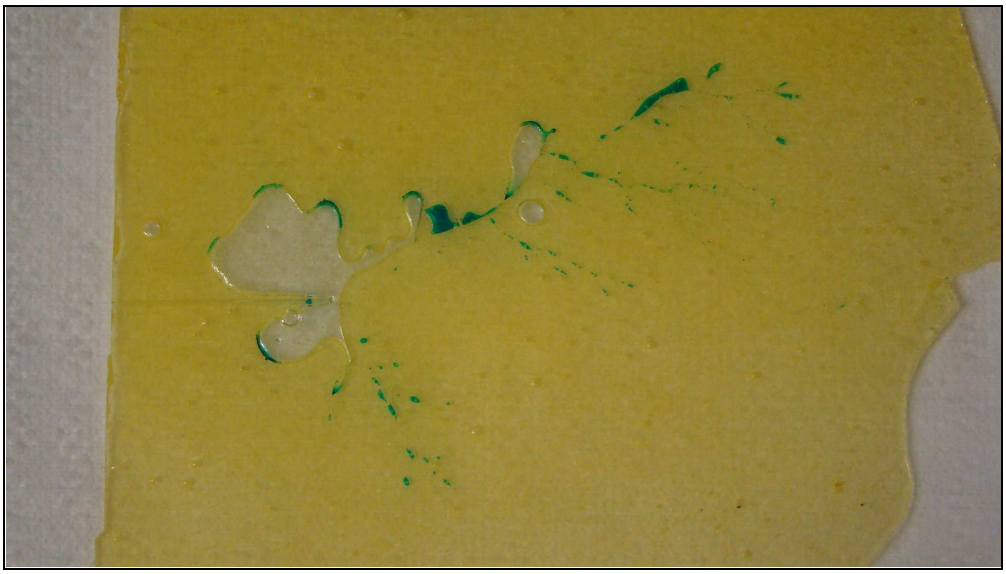

Figure 15: Cured CN-151/Styrene Branching Structure

There is a high degree of branching in this sample. However, the branches did not stay continuous during the run and droplets were formed prior to cure. This is due to the greater interfacial tension between vinyl ester and water than that of silicone oil and water. To compound this, no surfactant was added. The viscosity ratio for the study shown in Figure 15 is 1×10^{-5}, the Bond number is 2.96×10^{3}, and the capillary number is 6.03. As in the ebecryl example (Figure 13), the highly branched pattern is qualitatively supported with a Bond number greater than Ca, which is greater than one.

The electrical stresses are higher on this system, resulting in finer branches, yet the channels are less continuous due to the higher interfacial tension.

CHAPTER 6: EXPERIMENTS INVOLVING PRE-POLYMER MATRIX

6.1 Pre-Polymer Requirements

The exploratory research performed with the silicone oil and water system has shown that a number of matrix parameters are important in defining and controlling the growth of self-propagating branching structures. Finding a pre-polymer that fits the requirements for an electro-hydrodynamic Hele-Shaw flow allows for the replication of the results in the curable system.

The first requirement is that the matrix must be a dielectric. Electrical branching occurs only when a conductive material is injected into a non-conductive material. Branching structures are improved by increasing the electric stresses on the system, and this is done by increasing the potential across the cell. If the matrix carries a current, it would reduce the potential applied to the system.

The next requirement calls for a tunable matrix viscosity. This is vital in replicating the viscosity studies of the silicone oil and water system, and also in tailoring the degree of branching. For this, a reactive diluent added in varying concentration is needed.

The matrix material must exhibit Newtonian behavior, in which there is a linear relationship between the shear stress and the strain rate. This allows for the determination of a constant coefficient for the material's viscosity, which is important in determining

the capillary stress on the system. Non-Newtonian behavior would lead to unpredictable final branching patterns.

The chosen system must have the ability for rapid cure. This can be done by a timed cure or a UV-cure. Timed cure initiators limit the leisure of set-up for the researcher or production personnel. UV-cure is a viable option, since the existing set-up allows for the easy addition of a UV lamp. Thermal initiators are not an option, as heating the system tends to lower the viscosity, affecting the viscous fingering phenomena of the injection material.

The final requirement for the pre-polymer is for tailorable final material properties. It is important to have a final product which can either be rigid or flexible. These films may be used in a variety of applications which require different properties while still having a strong skin in order to contain the flowing injection material under stress.

6.2 Matrix Characterization

6.2.1 CN-151

Based on the requirements, the chosen material is a vinyl ester with a reactive diluent and UV-initiator. The vinyl ester chosen was CN-151 for its ready availability and widespread composite industry usage. CN-151 can also be diluted with a monomer while maintaining Newtonian behavior, and is a dielectric. Conductivity measurements were taken for all experimental materials using an Accumel Excel Conductivity Meter with a

range up to a thousandth of a µS. The standard solutions used to calibrate the instrument were 1.413 mS/cm and 84 µS/cm, making that the effective range for this experiment. The recorded conductivity for CN-151 was 0 µS/cm. CN-151 is also a desirable material, since it is rather flexible once cured, but rigid once it has been post-cured, allowing for tailorable properties. The chemical structure of CN-151 is shown in Figure 16.

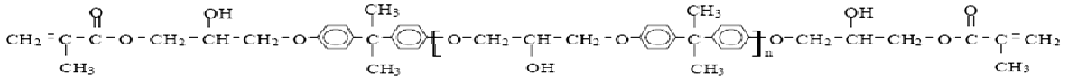

Figure 16: Chemical Structure of CN-151

6.2.2 Methacrylated Octanoic Acid

The reactive diluent used to tailor the viscosity of the matrix fluid is a methacrylated fatty acid that has been developed and patented by Drexel University. The specific material chosen is a methacrylated octanoic acid (MFA). Using the same conductivity meter as for the CN-151, both 100% MFA and a 31wt% MFA solution in CN-151 read as 0 µS/cm. MFA is a reactive diluent, participating in the cure of the vinyl ester. It also acts as a natural surfactant between the matrix and injection materials (CN-151 and water) because its molecular structure is hydrophilic at one end of the chain and hydrophobic on the other. The molecular structure of methacrylated octanoic acid is shown in Figure 17.

Figure 17: Chemical Structure of Methacrylated Octanoic Acid[20]

Adding MFA tailors the viscosity of the matrix solution. This was tested using a TA Instruments AR 2000ex rheometer with the corresponding rheology advantage software. Figure 18 shows the results of this study.

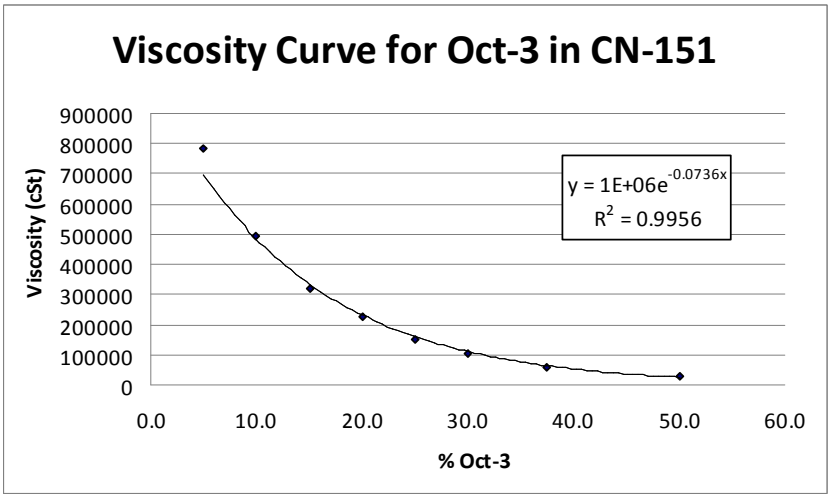

Figure 18: CN-151/MFA Viscosity as a function of MFA content at 25°C

The viscosity of the mixture decreases with an increase of the MFA content. The optimal branching structure in the silicone oil matrix was found at 100,000 cSt. Replicating the matrix viscosity of 100,000 cSt requires a 31 wt% MFA content in the CN-151.

---

[20] John J. LaScala, James M. Sands, Joshua A. Orlicki, Jason E. Robinette, and Giuseppe R. Palmese "Fatty acid-based based monomers as styrene replacements for liquid molding resins" *Polymer* vol. 45 (2004), p. 7729-737.

6.2.3 Initiator

Rapid cure of the matrix is required in order to freeze the branching structures in place before the system shorts and relaxes the channels created. To achieve this, 0.5 wt% camphorquinone and 0.5 wt% tetramethylaniline are used as UV-cure initiators in the matrix.

CHAPTER 7: PRE-POLYMER MATRIX RESULTS

The first point to make when examining the similarities and differences between the silicone oil and vinyl ester systems is that different ground leads were used for the two systems. In the silicone oil matrix experiments, a planar ground charge was used. This was a piece of copper tape that spanned the entire width of the cell and was affixed to the end farthest from the injection needle. In the vinyl ester matrix experiments, a point charge ground was used. This was an aluminum needle tip that was inserted at the end of the cell furthest from the injection needle. Both systems exhibit the same degree of branching and length scales between branches. The main difference is that the progress of the branching structure is much more spread out in the silicone oil system with the use of the planar charge, and has much more linear progress towards the point ground in the vinyl ester system. These differences can be noted by comparing the results of similar studies in both systems. Also note that the results of the polymer matrix are shown in black and white photos as opposed to color. Better visibility was obtained by presenting the data in this way, although the injection material is still a blue-dyed water and the matrix is still relatively clear as in the silicone oil experiments.

7.1 Effect of Viscosity Ratio

The viscosity ratio was systematically studied in the same manner as the silicone oil and water system. Vinyl ester viscosity was increased while applied voltage, injection flow rate, and injection material were maintained constant. The blue-dyed water was injected

at 0.2 mL/min with an applied potential of 45 kV. The top left picture of Figure 19 shows the injection of water into a 500 cSt pre-polymer matrix, which is 100% MFA. The top right picture shows the injection of water into a 1,000 cSt matrix, which is 93.3 wt% MFA. The injection of water into a 10,000 cSt matrix, which consists of 62.2 wt% MFA is seen in the middle left photo. The middle right photo shows the water injected into a 50,000 cSt pre-polymer, consisting of 40.5 wt% MFA. The bottom photo of Figure 19 shows the 100,000 cSt pre-polymer matrix designed to replicate the 100,000 cSt silicone oil results. This was created by mixing 31 wt% MFA with CN-151 vinyl ester.

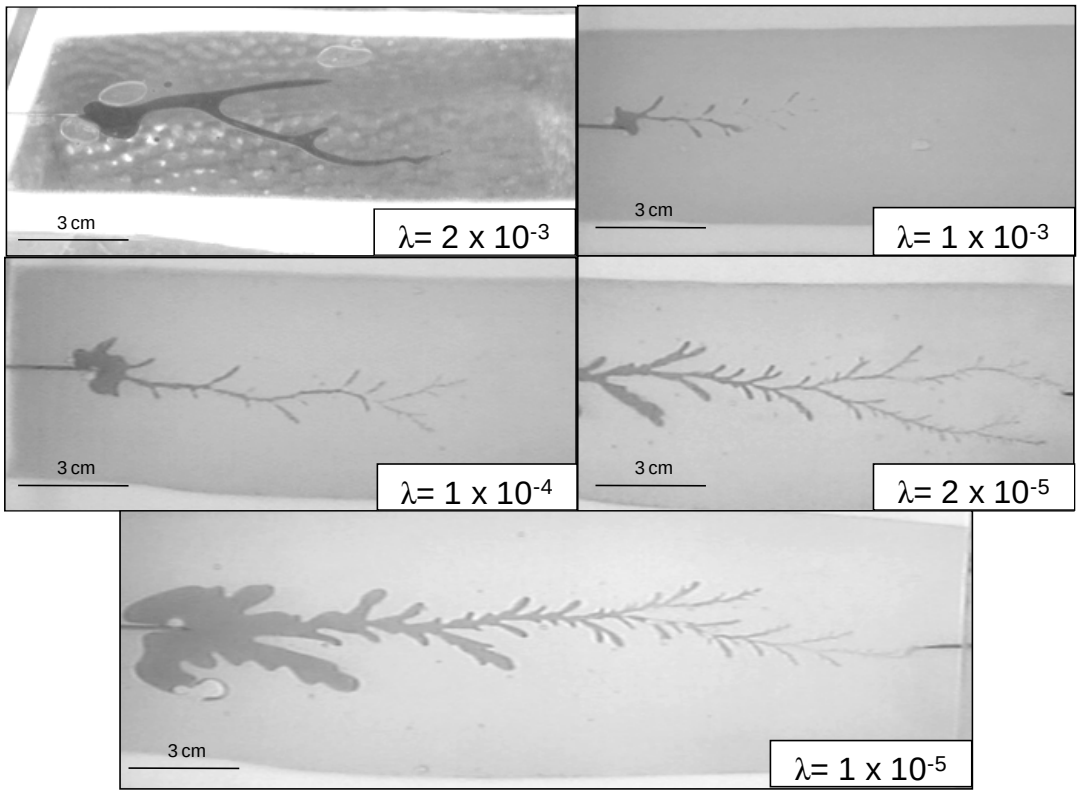

Figure 19: VE Viscosity Ratio Study Results

Qualitatively analyzing the results shows that the degree of branching increases with decreasing viscosity ratio. With increasing matrix viscosity, one can clearly see more branches in the structure formation.

A major difference between the silicone oil and vinyl ester systems shows no droplet formation when vinyl ester is used as the matrix material. The naturally occurring surfactant properties of the methacrylated fatty acid produces similar results in the vinyl ester system to that of silicone oil with surfactant added (Figure 6). With surfactant, the surface tension between the phases decreases and allows for continuous branching structures to form. This occurs even at higher viscosity ratios, which corresponds to lower capillary numbers. While the results can be qualitatively observed, the exact interfacial tension between the water and vinyl ester/MFA system is not known and therefore the capillary number is evaluated on an order of magnitude basis (Chapter 4.1), as seen in Table 12.

Table 12: VE Viscosity Study Dimensionless Analysis

λ	Bo	Ca
2.0E-03	5.4E+03	3.3E-01
1.0E-03	5.4E+03	6.6E-01
1.0E-04	5.4E+03	6.6E+00
2.0E-05	5.4E+03	3.3E+01
1.0E-05	5.4E+03	6.6E+01

The results show the dimensionless analysis on this study. As the viscosity ratio decreases, the capillary number increases while the Bond number stays consistent. This

analysis is the same as that done for the viscosity study of the silicone oil system shown in Table 6.

7.2 Effect of Voltage

The effect of voltage was systematically studied in the vinyl ester system in the same way that it was studied with the silicone oil matrix described in Chapter 4.2. However, experimental procedure was improved to the point where the system could be observed under a 60 kV applied potential as well, widening the range of possible experiments.

The experimental conditions that were set for this study were the injection flow rate of blue-dyed water at 0.2 mL/min and the vinyl ester matrix viscosity of 100,000 cSt. Applied voltage was changed incrementally to investigate the effect of the electric stresses on the system. Results for applied voltages of 0 kV, 15 kV, 30 kV, 45 kV, and 60 kV are shown in Figure 20.

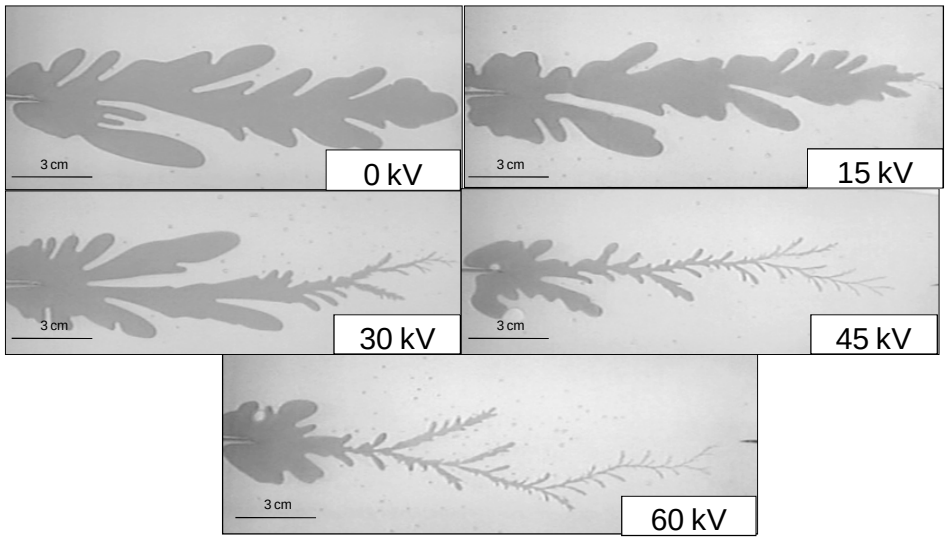

Figure 20: VE Voltage Study Results

Increasing applied potential across the cell decreases the length scale between the branches of the structure as seen in Figure 20. This is the same result that was obtained in the earlier silicone oil experiments (Table 10). Since the matrix fluid is a dielectric, but the injection material is conductive and all molecules are of the same polarity, any instability in a branch due to viscous fingering will create another branch. As the voltage increases, the electrical stress has an increasing effect on the branching pattern of the structure (Figure 20).

Table 13: VE Voltage Study Dimensionless Analysis

Voltage (V)	Bo	Ca
0	0.0E+00	6.6E+01
15	6.0E+02	6.6E+01
30	2.4E+03	6.6E+01
45	5.4E+03	6.6E+01
60	9.6E+03	6.6E+01

The dimensionless analysis shown in Table 13 proves that as the capillary and viscous stresses remain constant, increasing the voltage causes an increase in electric stresses. While the capillary number remains constant, the Bond number increases with increasing applied voltage. An increased Bond number corresponds to a decreased length scale between branches.

7.3 Effect of Flow Rate

The final parameter of the silicone oil studies that were replicated in the curable pre-polymer is the effect of injection material flow rate on the structure of the electrohydrodynamic branches. In this study, the parameters kept constant were a matrix viscosity of 100,000 cSt and 45 kV applied potential. The flow rate of the blue-dyed water is systematically increased to verify the effect of capillary number on the structure of the growth. The results can be seen in Figure 21.

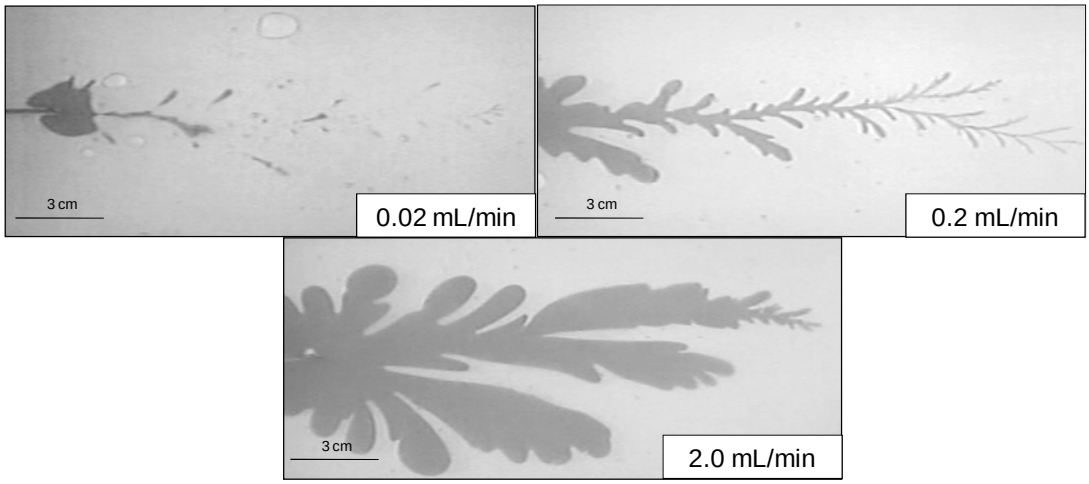

Figure 21: VE Flow Rate Study Results

The top left picture of Figure 21 shows a flow rate of 0.02 mL/min. Here, the capillary stresses have clearly overtaken the viscous stresses on the injection material, and while branches were created in the initial flow of water throughout the cell, they quickly closed due to forces exerted by the matrix material. The top right picture of Figure 21 shows the results of injecting the water at 0.2 mL/min. This shows a good balance between the stresses on the system, with a fine branching structure created. The capillary stresses are

less than the viscous stresses, which are less than the electric stresses. This is the optimal condition for a well-defined branching system. The bottom picture shows the results of injecting at 2.0 mL/min. At this point, material is being introduced into the system at a high flow rate, and the viscous stresses are high. As a result, pooling occurs in the branches that mimics viscous fingering without any applied electric potential. The fine branches are initially created, however the flow of material exceeds the original channel and creates the large pooled branches that are observed in Figure 21. These observations are supported by the dimensionless analysis completed for the experiment and displayed in Table 14.

Table 14: VE Flow Rate Study Dimensionless Analysis

U (m/s)	Bo	Ca
0.02	5.4E+03	6.6E+00
0.2	5.4E+03	6.6E+01
2	5.4E+03	6.6E+02

The series of pictures in Figure 21 shows the importance of minimizing the capillary stresses and tuning the viscous stresses on the system so that an optimal pattern can be obtained. The dimensionless terms summarized in Table 14 show quantitatively what is observed qualitatively in Figure 21. The best results are obtained at an intermediary capillary number while the Bond is kept constant. This reinforces the conclusion that the capillary number must be balanced in order to get the best branching and fill the channels without pooling.

7.4 Vinyl Ester Matrix Learnings

The second phase of this thesis work involved taking the principles discovered from the silicone oil studies (Chapter 4.5) and applying them to a curable system. This determined the applicability of the technology, and also tested the accuracy of the dimensionless analysis as a prediction tool for various matrix materials. The same array of studies were performed in the vinyl ester material as were done with the silicone oil.

In agreement with the silicone oil results, the capillary number of the vinyl ester system increases on an order of magnitude basis with decreasing viscosity ratio, while the Bond remains constant. Due to the increase of viscous stress, a higher degree of branching is seen as the matrix viscosity increases. This condition is systematically changed while the flow rate and voltage are maintained.

Increasing the voltage applied to the system also resulted in similar branching behavior to that in the silicone oil matrix. Matrix viscosity and flow rate remained constant, which kept the capillary number constant as the Bond number increased with increasing applied potential. The higher electric stress on the system results in a decreased length scale between the branches.

When the flow rate was systematically increased while all other process conditions were kept the same, the capillary number increased as the Bond remained constant. As Ca increased, the pooling within the branches became much more prevalent.

Flow studies completed in the vinyl ester matrix confirmed the silicone oil results and conclusions. Consistently well-defined and well-branched channels were created with a high matrix viscosity, a high applied voltage, and a tailored injection flow rate. This corresponds to the same dimensionless analysis that was used to predict branching patterns in the silicone oil system. The viscosity ratio must be as low as possible to minimize the inertial stress on the system. The electric stress must be higher than the viscous stress, which in turn must be higher than the capillary stress for optimal branch formation. These stresses correspond to a Bond number which is greater than the capillary number, which is greater than unity.

Consistently creating well-defined branches within a pre-polymer system is the precursor to curing the channels in place. The ability to apply the dimensionless terms to multiple types of systems opens processing capabilities to other novel pre-polymer materials. The success of predicting structure formation in these two materials demonstrates the general functionality of the method.

CHAPTER 8: *IN-SITU* CURE OF VINYL ESTER SYSTEM

8.1 Equipment

The procedure for creating a branching structure and curing it into place is relatively simple. The only alteration to the original flow procedure is the addition of photoinitiator to the pre-polymer, and the application of a UV light during the run. The set up required for this experiment is shown in Figure 22.

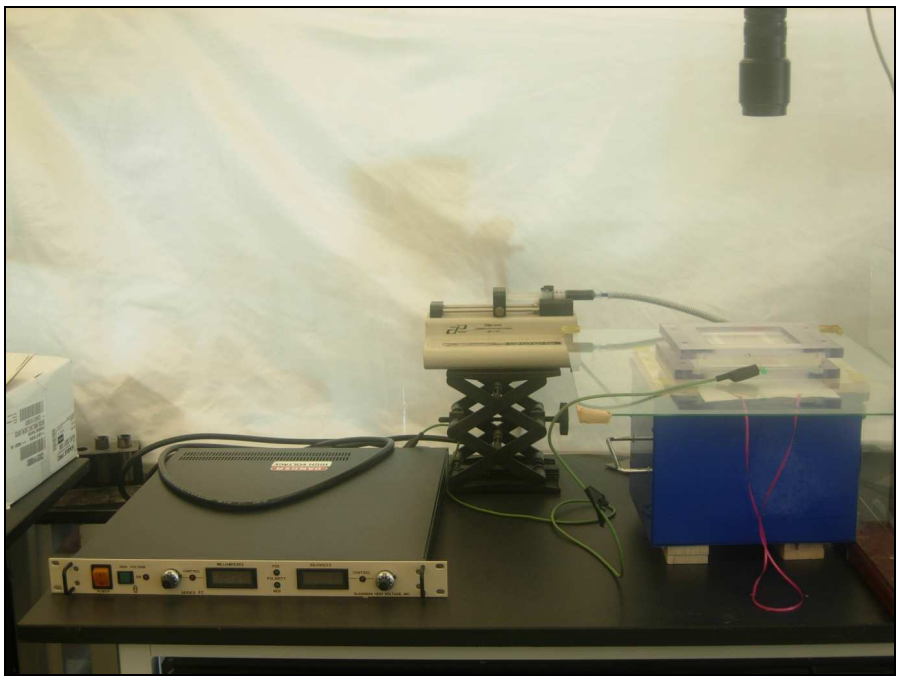

Figure 22: UV-Cure Experimental Setup

To the left of the lab bench is the high voltage source. This model is manufactured by Glassman High Voltage, Incorporated. It has a 115 AC input and a -60 kV output. It is limited to a current of 2.0 mA. The scissor lift in the middle of the picture is holding a

syringe pump that has a wide range of outputs. A 10 mL syringe is used to hold the injection material, which is blue-dyed water for all experiments. The syringe pump is electrically isolated by a long piece of plastic PEEK tubing. The distance between the cell and the syringe pump is approximately one foot long. The blue box at the right side of Figure 22 is the UV light source. This is electrically isolated from the experimental cell by a 1/8 inch sheet of glass. A shutter is installed which allows for the control of light exposure to the sample. The light being emitted from this source was measured to be 11.5 mW/cm^2 of blue light and 2 mW/cm^2 of UV-A above both the insulating plate glass and the glass cell layer (at the sample surface). The sample cell is located above the sheet glass. A camera is suspended above the entire set up so that the qualitative data can be collected for each run. The camera has both video and still picture capabilities at a high resolution.

Figure 23 shows a close-up of the Hele-Shaw flow cell that is used for this experiment. It is electrically isolated to deliver accurate potential across the cell.

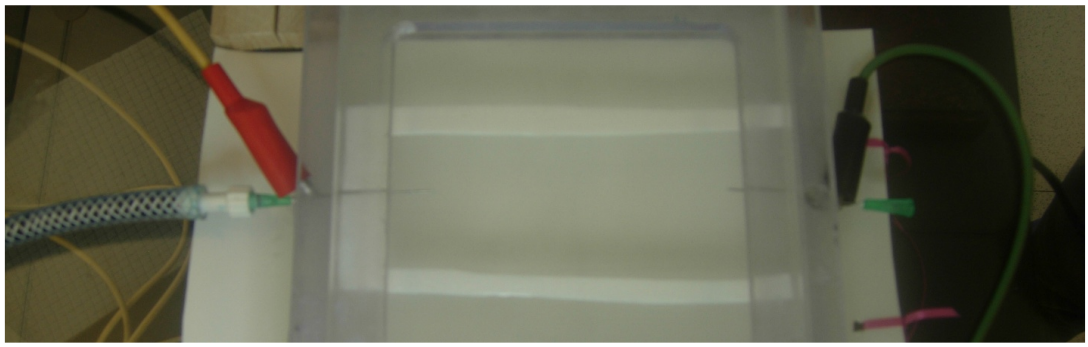

Figure 23: Close-up of UV-Cure Hele-Shaw Cell

Figure 23 is very similar to the Hele-Shaw cell used for the silicone oil experiments. The same dimensions and gasket material are used for this model. However, the material of the new cell is ½" thick float glass rather than polycarbonate. A polycarbonate frame is used to tighten the two pieces of glass together to the height of the spacer shims.

Glass is used for the cell for a few reasons. First, vinyl ester must be cleaned with acetone, which eats away at the polycarbonate. Also, polycarbonate blocks UV light while glass does not. Using glass allows for the UV cure of the vinyl ester system. Glass also exhibits the same dielectric properties as polycarbonate, and does not flex under the stress of the bolts used to tighten the plates together. The hot lead is attached to the injection needle, and the ground lead is attached to a ground material in the same way that the silicone oil experiments were set up.

Figure 24 shows the side view of the *in-situ* cure equipment set-up. Note the only change between the silicone oil experiments and the curable pre-polymer set up is that the matrix material is vinyl ester and MFA, the cell is made from float glass plates, and a UV light source emits from below the cell.

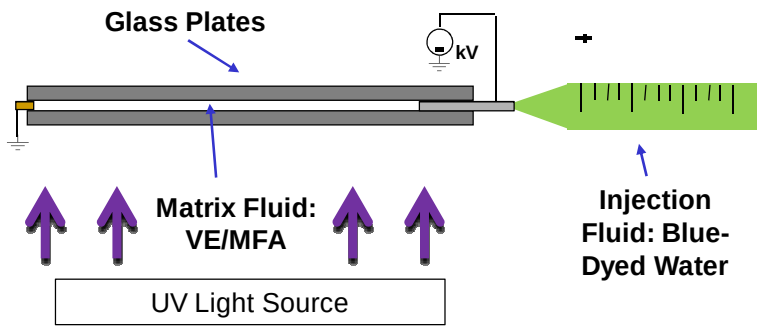

Figure 24: UV-Cure Hele-Shaw Cell Schematic

8.2 Experimental Procedure

The *in-situ* cure of the branching structures is accomplished by adding a UV-cure agent to the matrix and then exposing the pre-polymer to light. The timing of the light application is a variable that must be finely tuned. If the system cures too quickly, it becomes sealed and there is no place for the injected water to flow. This causes a back up of the system where water flows out through the gasket. Water then shorts to the injection needle. If the system cures too slowly, the water shorts once it reaches the ground lead and causes relaxation of the finest branches that have been created. Relaxation occurs because electrical stress is removed from the system at shorting The most consistently effective way of curing the system is to remove the shutter along the same timeline as the progress of the flow pattern. When the light is exposed to existing branches as they form, they are locked in place. This also minimizes the amount of material that is uncured once the system shorts, so the branches will not relax since they have already been cured in place.

The most successful results have been obtained with a 100,000 cSt matrix viscosity, an 0.2 mL/min injection flow rate, 60 kV of applied electric potential, and applying the UV light to the cell by following the growth speed with the shutter opening. The procedure for this successful experiment is outlined in section 8.2.1.

8.2.1 Experimental Procedure

I. Obtain 20 g of matrix material

i. 31 wt% MFA, or 6.2 grams

ii. 0.5 wt% Camphorquinone, or 0.1 grams

iii. 0.5 wt% Tetramethylaniline, or 0.1 grams

iv. 68 wt% CN-151 vinyl ester, or 13.6 grams

II. Obtain injection material

i. 10 drops of blue McCormick food coloring per 50 mL of tap water

III. Fill the syringe set-up

i. First fill the electrically isolating tubing with blue-dyed water

ii. Next attach a 10 mL syringe and fill with blue-dyed water

iii. Eliminate any air bubbles in the set up

IV. Set up the Hele-Shaw cell

i. Insert a gasket made of closed-cell foam. This research used FDA Polyethylene Foam 1/16 inches thick. The inner dimensions of the gasket are 3” x 5.5”.

ii. Spray the glass plates with PTFE release spray.

iii. Fill the gasket with the matrix material.

iv. Affix the injection needle to one end of the flow cell after priming the needle.

v. Attach the positive lead to the injection needle.

vi. Insert a ground lead attached to the ground of the high voltage source.

vii. Affix spacers of the same height as the injection needle and tighten the cell until the height of the matrix is the same as these spacers.

V. Turn on the UV lamp with the shutter in place.

VI. Apply voltage to the cell. Ensure that the ground is firmly connected to the high voltage source, and that the amps are limited to very low. Slowly raise the voltage. The best results were found at a 60 kV potential.

VII. Turn on the syringe pump to the desired flow rate. Best results were found at 0.2 mL/min.

VIII. Turn on the camera for video footage of the run.

IX. Slowly open the shutter to the UV lamp to follow the progress of the branching structure. This will freeze the pattern in place.

X. Turn off the voltage at the moment the water reaches the ground lead and shorts.

XI. Slowly open the cell and pry the cured polymer film from the glass plates.

XII. Postcure if desired.

8.3 Cured System Results

Curing the system was done by applying UV light to the polymer at difference stages of injection. Differing the timing resulted in varied structures, which are given below.

8.3.1 Premature Cure

As mentioned in section 8.1, exposing the system to UV light too soon will cure the matrix and cause backflow of the injected material. All process conditions mentioned in the procedure were maintained in this experiment. The matrix is 100,000 cSt MFA/CN-

151 with 0.5 wt% each of camphorquinone and tetramethylaniline. 60 kV was applied and the water was injected at 0.2 mL/min. The results can be seen in Figure 25.

Figure 25: Premature Cure Example

Figure 25 shows a cured polymer with very little branching. This is due to the fact that the UV light was applied at the beginning of the injection, and the system cured too quickly to allow for fluid transport through the matrix.

8.3.2 Late-Stage Cure

On the other hand, the system can be exposed to UV light when the water has almost reached the ground. Following this procedure can create well-defined structures, as seen in Figure 26. However, there is a risk in waiting this long to begin cure. If the system shorts before channels are cured in place, more relaxed structures are formed, since the fine branches are no longer holding their position without the presence of electric stress.

All process conditions shown in Figure 26 were kept constant with the outlined procedure. Shutter timing was the only change.

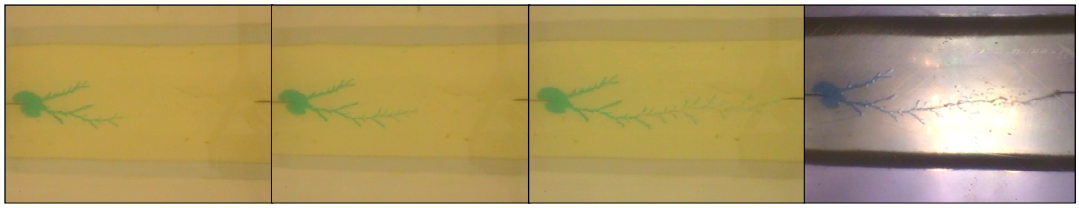

Figure 26: Late-Stage Cure Example

Figure 26 shows the progression of the fluid injection and branching in the polymer system, and the application of UV light at the end of the run. A thinly branched channel is created, which has a high degree of branching. The risk with this method is the relaxation of the branches. If the polymer were to cure too slowly and the electrical circuit were to short before a channel was created, finely branched structures would not be set in optimal configuration within the polymer.

8.3.3 In-Process Cure

Figure 27 shows the results of the same experimental parameters as described in the procedure and in earlier results. The shutter follows the flow of the water throughout the cell and therefore cures the branches in place as they are formed in this variation of the experiment.

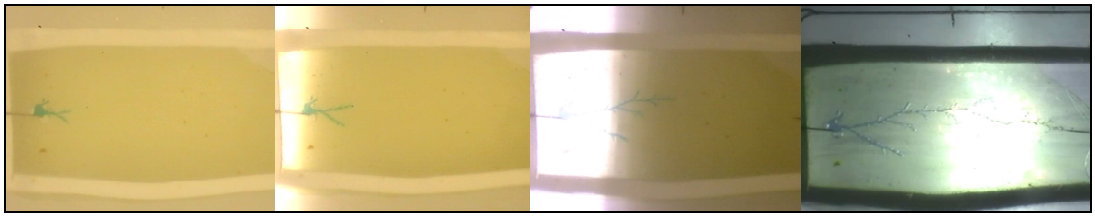

Figure 27: In-Process Cure Example

Figure 27 shows the technique of using the shutter to follow the flow of the branches and to cure the sample as it is created. This results in the most consistently formed pieces, since there is reduced risk of curing the matrix too quickly so that the injection material can't flow, or of curing the matrix too slowly so that the system shorts electrically. However, successful samples were fabricated using all three curing techniques. The parameters that remained constant for all of these methods were the 0.5 wt% tetramethylaniline and 0.5 wt% camphorquinone photo initiators, and the UV light intensity supplied by the same source. UV cure is an effective means for quickly polymerizing the sample and freezing the branched channels in place.

Figure 28 shows an example of a fully cured system. Note the density of small length-scale branches that was achieved. This is an example of a well-formed self-patterned branching structure within a polymeric material.

Figure 28: Well-Defined Branched Structure in Vinyl Ester Matrix

Figure 28 shows the results of a sample that was cured when the water was very close to completing the circuit and shorting out. The matrix material is 100,000 cSt vinyl ester achieved by diluting CN-151 with 31 wt% methacrylated octanoic acid. The applied electric potential is 60 kV across the cell and the injection rate of the blue-dyed water is 0.2 mL/min. The fine branches produced are fully encased by polymer. This method does have a higher risk of creating relaxed branches. However, it has also met with success. The consistently successful results were obtained through in-process cure.

There are a number of variables that affect the cure of the system. The increasing concentration of photoinitiator system camphorquinone and tetramethylaniline will decrease the amount of time required to cure the pre-polymer. Heating the matrix material will not only decrease the viscosity, but it will also release more free radicals and again, decrease the amount of time required to cure the matrix. The amount of time that the sample is exposed to light during setup also affects its curing time during the experimental run. Therefore it is important to quickly set up the sample, and to keep it out of the light as possible.

A high-quality shutter installed on the UV lamp precisely controls the exposure to the sample. Since UV lamps take time to warm up, the sample can be exposed to low levels of light without a shutter in place. The shutter also allows for controlled exposure time during the run.

8.4 Fluid Fill and Flow Through Cured Systems

Successfully creating branching structures and freezing them in place into a polymeric film leads to the potential applications of these free-forming vascular systems. However, achieving fluid fill and flow throughout the channels is required in order to realize different applications. It has been successfully demonstrated that finely and far-reaching branching structures can be created on a consistent basis. It has also been shown that these structures can be re-created in vinyl ester systems and cured in the same form that they were originally created. These branches truly do create a channel through the polymer, with a thin film on either side of the structure. The film created is flexible before post cure and rigid after heating to 90°C for 30 minutes. In either case, the channels are permanent structures within the film.

Capillary action was not a successful method in re-filling the branches. It was discovered that a pressure differential is required to draw material into the small cavities of the channel. This is helpful in potential applications. Since “wicking” a material from a crack-site draws vacuum and causes a pressure differential across the channel, it will draw more fluid into the branch and in that way deliver material to a fault in a polymer or composite. This is helpful in self-healing material applications, where a monomer will be

held in the branched channels. Once a crack propagates on the surface, the monomer will spill out of the channel and polymerize. This will cause a pressure differential, drawing more monomer from a reserve and out to the crack site. The process will continue until the crack is sealed.

The wicking of material from the crack was used to create a pressure differential in experimentation. Simultaneously, a fluid was injected into the branches. Here, red-dyed water and blue-dyed water were alternately injected into a sample. Figure 29 shows the progression of flow through the larger branches of the one structure. This was an early flow experiment that showed proof of concept at a large branch scale. Time of injection progresses from left to right.

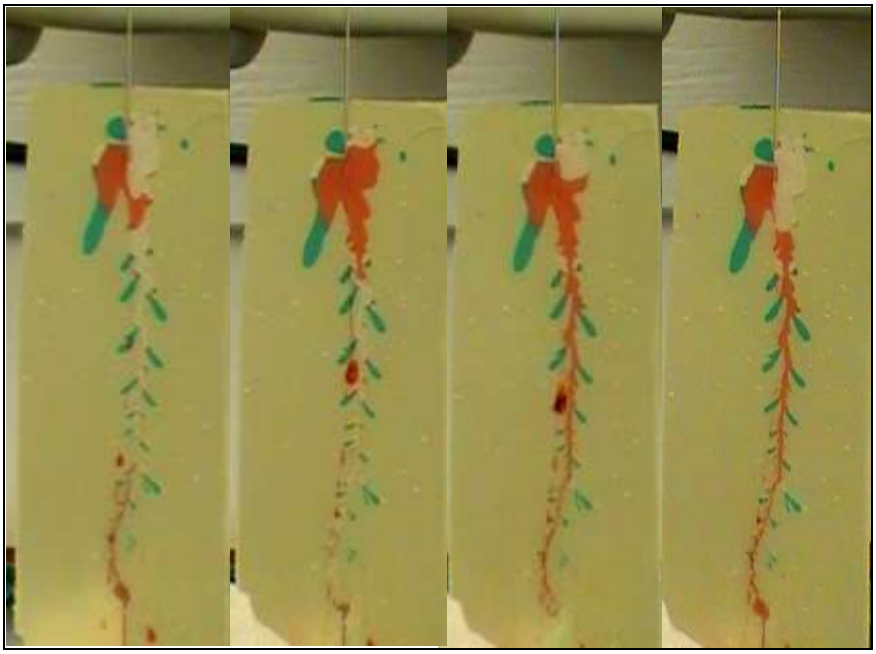

Figure 29: Fill and Flow Sequence Through Large Length Scales

You can see the draining of liquid in the first picture as it is being wicked away. The second picture shows the injection of new material into the channels. The third picture shows the complete fill of the branch, and the last photo shows the fluid flow as the chamber at the top of the sample begins to empty again.

Fluid fill and flow was also successfully demonstrated on a smaller branch scale. This was done by cutting a cured system so that the opening to a smaller branch could be reached. The same process was repeated. A paper towel was used to wick the existing fluid out of the channel while another colored fluid was simultaneously injected via a needle and syringe apparatus. As in earlier tests, material was successfully injected, removed, and replaced multiple times within the same branched channel. The channels easily held up to this material movement and to the handling required in order to accomplish the experiment. Figure 30 shows the progression of flow through this smaller branch scale, again, with time progressing from left to right.

Figure 30: Fill and Flow Sequence Through Small Length Scales

Note the complete fill of the main branch as it is wicked from the outlet in Figure 30. The first photo shows the beginning of the injection, with a small bead being formed at the bottom of the sample. The second photo shows the material mixing as the red is injected into the blue. The third shows the displacement of the blue water out of the sample, and the fourth shows the fill of the branches with red water as well as the displacement of that red material from the sample.

Figure 31 shows the fill of an even smaller length scale. The sample used for the results shown in Figure 30 is re-used in this experiment. The side branches of this piece are being filled with red-dyed water.

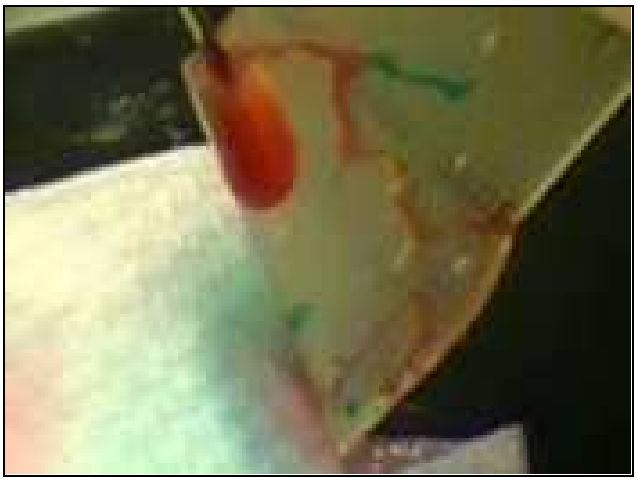

Figure 31: Fluid Flow Through Smallest Achieved Length Scale

The complete fill of these channels and the red stain on the paper towel indicate that the new material has flowed completely through the sample.

Figure 32 zooms in on this same sample to show the degree of fluid fill that was achieved in this experiment. Once the wicking material is removed from the channel outlet, it is possible to completely refill the branches.

Figure 32: Completed Fill of Branched Structure

The one blue branch which is left in Figure 32 shows the importance of creating a pressure differential across the channel in order to force new material into the space. This blue branch does not lead to an outlet at the edge of the sample, as all the red branches do. There is no location for the blue-dyed water to flow towards in order to be replaced by red.

Dyed water was the selected material for these preliminary flow studies. However, any material that is low in viscosity would be appropriate for this network. Low viscosity is required so as not to plug the branches, which are no more than 0.8 mm in diameter. This transport method is appropriate for low viscosity materials such as monomers, coolants, and dyes. With monomers, self-healing applications of polymers or composites can be

achieved. With coolants, temperature control or heat transfer can be achieved through this material. And finally, with dyes, property modification of the polymer or damage detection can be achieved.

CHAPTER 9: CONCLUSIONS AND FUTURE WORK

9.1 Conclusions

It has been determined that branching structures in pre-polymeric systems can be achieved by combining the phenomena of viscous fingering and electrical treeing. Preliminary work in defining these branching structures has been conducted. The pertinent stresses that affect the system are now understood and their qualitative effects on structure formation can be predicted with the use of dimensionless analysis. Electric, viscous, and capillary stresses combine to form the Bond and capillary numbers. In order to have a well-defined branching structure with a large quantity of highly dense branches, the Bond number must be larger than the capillary number, which must be greater than unity. This corresponds to an electric stress that is higher than the viscous stress, which is in turn higher than the capillary stress on the system. This is achieved with a high electric potential applied to the system, a high matrix viscosity and low injection viscosity, and a tailored, intermediate flow rate of the material being injected. Low interfacial tension between the two phases makes the structures achievable under these conditions.

The *in-situ* cure of branched structures has also been achieved, creating branched channels capable of fluid transport. This was done by first tailoring the viscosity of vinyl ester resin CN-151 with the addition of the reactive monomer, methacrylated octanoic acid, and then UV curing the structure during the injection process using an appropriate photoinitiator. By wicking the un-reacted injection material (water) out of a crack in a branch, it was possible to inject new material into the channels. It was found that this can

be done throughout a wide range of channel dimensions, and can be used to create both fluid flow and fill of the branches. The channels were found not to be affected by this process, and maintained their cured size and shape through multiple injections.

9.2 Future Work

The work summarized in this thesis is a proof of concept for the electro-hydrodynamic method of creating self-patterning branched structures. The scope of the work included characterizing flow, using the characterization to control the flow, creating permanently branched channels in a polymeric system, and obtaining liquid fill and flow of those channels. In order to apply this academic concept for use within an application, continued study and experimentation of the system is recommended. The following outlines some of the future work that has been identified throughout this study.

9.2.1 Branching Characterization

Preliminary studies have been completed for characterizing the branching structures created with electro-hydrodynamic flow through a Hele-Shaw flow cell. The dimensionless analysis that has been completed takes all stresses in the system into account, but is analyzed on an order-of-magnitude basis only. This is mainly due to the fact that the exact interfacial tension between the two materials is not exactly known, and must be estimated. Finding a reliable method for determining interfacial tension between the matrix material and the injected material is a future work that will make the dimensionless analysis more exact, and more reliable when used to determine the

behavior of a branching system. The dimensionless analysis also does not take inertial stresses into account. While it is hypothesized that the capillary, electric, and viscous stresses overtake the inertial stresses, there is scientific value in determining the inertial stress and its effect on the branching patterns.

The pre-polymer matrix used in this series of experiments was created by mixing vinyl ester CN-151 with a reactive monomer, methacrylated octanoic acid. However, an entire series of methacrylated fatty acids have been synthesized at Drexel University, and using an MFA with a longer carbon chain would increase the surfactant effect of the diluent and reduce the interfacial tension between the two phases by an even greater amount. Experimentation using these materials in this process will help to determine the effect of interfacial tension, and may yield superior branching results.

9.2.2 Curable Systems

Creating a reliable cured system was completed within the scope of this thesis. Preliminary work with directing the flow has also been completed. Further work in directing the flow via placement of electric leads or application of pressure can be done to further the applicable uses of the technology.

All polymeric systems created in the scope of this work were done in the Hele-Shaw cells of the same dimension. Different types of leads, including planar and point leads, have been experimented with. Future work to be explored in this area needs to be done with scaling of the technology to encompass both smaller and larger dimensions. In

application, the branching patterns will need to successfully scale, depending on the size of the cell and the desired coverage area.

9.2.3 Interfacial Polymerization

Many techniques are available for curing branching structures into a polymerized product. While UV cure was the first method attempted, interfacial polymerization between the two phases is another feasible alternative. By adding sebacoyl chloride to the organic phase (the matrix fluid) and hexamethylene diamine to the aqueous phase, a polymerized nylon shell should form between the two. This is similar to the techniques used for microencapsulation used in the pharmaceutical and food industries.[21]

9.2.4 Active Modulation for Tailored Structures

Currently, control of the flow of the system is possible with the placement of positive leads along the cell. The goal is to actively change the processing conditions throughout the flow in order to obtain more complex patterns. This can be done by adjusting flow rate, applied voltage, and location of point charges in time throughout the run.

9.2.5 Potential Applications

The main drive for a controllable biomimetic vascular structure within a material is to achieve the ability for modifiable properties of structures. Vascular systems can be used for self-healing of composites and polymers. The materials affected can vary from load-

[21] Benita, Simon. Microencapsulation: Methods and Industrial Applications. Vol. 73. Informa Health Care, 1996.

bearing composite structures to flexible materials used for personal protective equipment. Active color-change within a polymer or for damage detection is another use for this technology. These channels could be used in cooling systems, microreactors, or to change the surface properties of polymeric systems.

More importantly, these branched structures are relatively inexpensive to create, the growth is controllable for the desired system shape, and this technology can be easily scaled for multiple matrices. The opportunities for applying these branching systems are vast and with the development of increasingly sophisticated composite systems, will have infinite applications.

List of References

1. Benita, Simon. Microencapsulation: Methods and Industrial Applications. Vol. 73. Informa Health Care, 1996.

2. Bond, IP, and JWC Pang. "Bleeding Composites- Damage Detection and Self-Repair Using a Biomimetic Approach." Composites 36 (2005): 183-188.

3. Cardona, F, D Rogers, S Davey, and G Van Erp. "Investigation of the Effect of Styrene Content on the Ultimate Curing of Vinylester Resins by TGA-FTIR." Journal of Composite Materials 41 (2006): 137-152.

4. Chanson, Hubert. Hydraulics of Open Channel Flow: An Introduction. 2nd ed. Oxford [UK]: Elsevier Butterworth Heinemann, 2004. Print.

5. *Ciba Specialty Chemicals*. Web. 20 Oct. 2009. <http://www.ciba.com>.

6. Dodd, SJ. "A Deterministic Model for the Growth of Non-Conducting Electrical Tree Structures." Journal of Physics D: Applied Physics 36 (2002): 129-141.

7. Emerson, David R., Krzysztof Cies´licki, Xiaojun Gua, and Robert W. Barbera. "Biomimetic Design of Microfluidic Manifolds Based on a Generalised Murray'S Law." Lab on a Chip 6 (2006): 447-454.

8. Kanellopoulos, AG, and MJ Owen. "The Adsorption of Polydimethylsiloxane Polyether ABA Block Copolymers At the Water/Air and Water/Silicone Fluid Interface." Journal of Colloid and Interface Science 35 (1970): 120-125.

9. LaScala, John J., James M. Sands, Joshua A. Orlicki, Jason E. Robinette, and Giuseppe R. Palmese. "Fatty acid-based based monomers as styrene replacements for liquid molding resins." Polymer 45 (2004): 7729-737. Print.

10. Lide, David R., ed., CRC Handbook of Chemistry and Physics, Internet Version 2007, (87th Edition), <http:/www.hbcpnetbase.com>, Taylor and Francis, Boca Raton, FL, 2007.

11. Park, CW, and GM Homsy. "The Instability of Long Fingers in Hele-Shaw Flows." Physics of Fluids 28 (1985): 1583-1585.

12. *Sigma Aldrich*. Web. 20 Oct. 2009. <http://www.sigmaaldrich.com>.

13. Tabeling, P, G Zocchi, and A Libchaber. "An Experimental Study of the Saffman-Taylor Instability." Journal of Fluid Mechanics (1986): 67-82.

14. Therriault, Daniel, Scott R. White, and Jennifer A. Lewis. "Chaotic Mixing in Three-Dimensional Microvascular Networks Fabricated by Direct-Write Assembly." Nature (2003).

15. Therriault, Daniel, Scott R. White, Jennifer A. Lewis, and Robert F. Shepher. "Fugitive Inks for Direct-Write Assembly of Three-Dimensional Microvascular Networks." Advanced Materials 17 (2005): 395-399.

16. Trask, RS, IP Bond, and GJ Williams. "Bioinspired Self-Healing of Advanced Composite Structures Using Hollow Glass Fibres." Journal of the Royal Society Interface 4 (2006): 363-371.

17. Vaughn, AS, et al. J. Mat Sci. v39 p181-191. 2004.
Vaughn, AS, SJ Dodd, and SJ Sutton. "Raman Microprobe Study of Electrical Treeing in Polyethylene." Journal of Materials Science 39 (2004): 181-191.

18. Welty, James, and Charles E. Wicks. Fundamentals of Momentum, Heat, and Mass Transfer. New York: Wiley, 2001. Print.

19. Wilkes, James O. Fluid Mechanics for Chemical Engineers. 2nd ed. Upper Saddle River, N.J: Prentice Hall PTR, 1999. Print.